General Disclaimer

One or more of the Following Statements may affect this Document

- This document has been reproduced from the best copy furnished by the organizational source. It is being released in the interest of making available as much information as possible.

- This document may contain data, which exceeds the sheet parameters. It was furnished in this condition by the organizational source and is the best copy available.

- This document may contain tone-on-tone or color graphs, charts and/or pictures, which have been reproduced in black and white.

- This document is paginated as submitted by the original source.

- Portions of this document are not fully legible due to the historical nature of some of the material. However, it is the best reproduction available from the original submission.

Produced by the NASA Center for Aerospace Information (CASI)

School of
ENGINEERING
DUKE UNIVERSITY

(NASA-CR-157474) MEASUREMENT TECHNIQUES FOR THE CHARACTERIZATION IN THE FREQUENCY DOMAIN OF REGULATED ENERGY-STORAGE DC-TO-DC CONVERTERS M.S. Thesis (Duke Univ.) 111 p HC A06/MF A01 CSCL 10C G3/33 N78-29349 Unclas 27232

MEASUREMENT TECHNIQUES FOR THE CHARACTERIZATION IN THE FREQUENCY DOMAIN OF REGULATED ENERGY-STORAGE DC-TO-DC CONVERTERS

by

David Dean Bahler

Dept. of Electrical Engineering
Duke University
Durham, N.C. 27706

Prepared under Research Grant No. NGL 34-001-001, Supplement 17

August 16, 1978

MEASUREMENT TECHNIQUES FOR THE CHARACTERIZATION IN THE FREQUENCY DOMAIN OF REGULATED ENERGY-STORAGE DC-TO-DC CONVERTERS

by

David Dean Bahler

Department of Electrical Engineering
Duke University

Date: August 16, 1978

Approved:

Harry A. Owen, Jr. Supervisor

Devendra P. Garg

Thesis submitted in partial fulfillment of the requirements for the degree of Master of Science in the Department of Electrical Engineering in the Graduate School of Arts and Sciences of Duke University

ACKNOWLEDGEMENTS

The research was supported by Research Grant NGL-34-001-001 from the National Aeronautic and Space Administration, Washington, D.C. to Duke University.

I would like to express my deepest appreciation to my professors Dr. Harry A. Owen, Jr. and Dr. Thomas G. Wilson for their invaluable assistance in the research and preparation of this manuscript and for their understanding patience and inspiration during my two years of graduate study at Duke University.

I would like to thank Mrs. Margrid Casseday for the typing of this thesis and Mr. Jimmy Hartley for the drafting included in these pages.

Finally, I would like to thank my parents for pointing me in the proper direction and my good friend Zeke for his unwavering loyalty and faith in even the most difficult of situations.

TABLE OF CONTENT

ACKNOWLEDGEMENTS ii

LIST OF FIGURES iv

LIST OF TABLES vii

I. INTRODUCTION 2

II. ANALYTICAL DERIVATION OF CONVERTER SMALL-SIGNAL TRANSFER FUNCTIONS 5

Power Stage Transfer Functions, 5
Feedback Controller Transfer Functions, 15

III. EXPERIMENTAL MEASUREMENT PROCEDURES 26

Introduction, 26
Loop Gain, 32
Output Impedance, 37
Closed-Loop Gain, 42
Audio Susceptibility, 47

IV. EXPERIMENTAL AND ANALYTICAL RESULTS AND COMPARISON 52

Introduction, 52
Constant-Frequency Voltage Step-Up Converter (FQVU) Operating in the Continuous Conduction Mode (Mode 1), 59
Constant-Frequency Voltage Step-Up Converter (FQVU) Operating in the Discontinuous Conduction Mode (Mode 2), 68
Constant-Frequency Current Step-Up Converter (FQCU) Operating in the Continuous Conduction Mode (mode 1), 77
Constant-Frequency Current Step-Up Converter (FQCU) Operating in the Discontinuous Conduction Mode (Mode 2), 86
Discussion, 95

V. CONCLUSION 97

LIST OF REFERENCES 100

BIOGRAPHY 102

LIST OF FIGURES

FIGURES		PAGE
2.1	Circuit model and state variable waveforms for a small-signal analysis of the constant frequency voltage step-up converter	7
2.2	Constant-frequency feedback controller used in experimental converters of chapter IV.	16
2.3	Resistive attenuator network of figure 2.2	17
2.4	Error amplifier network of figure 2.2	19
2.5	Straight line approximation of triangle wave generator of figure 2.2 with an arbitrary error voltage of 4.0 Volts. Corresponding on-time and off-time indicated below.	20
2.6	Oscillogram of the output of the triangle wave generator taken from the circuit of figure 2.2	21
2.7	Oscillogram of the triangle wave generator and error voltage with the corresponding base drive on-time and off-time indicated below. Oscillogram taken from circuit of figure 2.2 A: Triangle wave generator, B: Error voltage, C: Base drive current	22
2.8	Time graphs for the derivation of the gain of the pulse-width-modulator of the circuit of figure 2.2	24
3.1	Diagram for the derivation of the output impedance of a regulated dc-to-dc converter.	29
3.2	Layout diagram for the measurement of loop gain.	32
3.3	Layout diagram for the measurement of output impedance	37
3.4	Layout diagram for the measurement of closed-loop gain	42
3.5	Layout diagram for the measurement of audio susceptibility	47
4.1	Power stage of the constnat-frequency voltage step-up converter (FQVU) used with the controller of figure 2.2 for experimental-analytical comparison	54

4.2	Power stage of the constant-frequency current step-up converter (FQCU) used with the controller of figure 2.2 for experimental-analytical comparison	55
4.3	The configuring of the frequency dependent blocks within the computer analysis	57
4.4	Loop gain of a constant-frequency voltage step-up converter operating in the continuous conduction mode. Power stage of figure 4.1, controller of figure 2.2	61
4.5	Output impedance of a constant frequency voltage step-up converter operating in the continuous conduction mode. Power stage of figure 4.1, controller of figure 2.2. Output impedance in dB referenced to 1 Ω	63
4,6	Closed-loop gain of a constant-frequency voltage step-up converter operating in the continuous conduction mode. Power stage of figure 4.1, controller of figure 2.2	65
4.7	Audio susceptibility of a constant-frequency voltage step-up converter operating in the continuous conduction mode. Power stage of figure 4.1, controller of figure 2.2	67
4.8	Loop gain of a constant-frequency voltage step-up converter operating in the discontinuous conduction mode. Power stage of figure 4.1, controller of figure 2.2	70
4.9	Output impedance of a constant-frequency voltage step-up converter operating in the discontinuous conduction mode. Power stage of figure 4.1, controller of figure 2.2. Output impedance in dB referenced to 1 Ω	72
4.10	Closed-loop gain of a constant-frequency voltage step-up converter operating in the discontinuous mode. Power stage of figure 4.1, controller of figure 2.2	74
4.11	Audio susceptibility of a constant-frequency voltage step-up converter operating in the discontinuous conduction mode. Power stage of figure 4.1, controller of figure 2.2	76

4.12	Loop gain of a constant-frequency current step-up converter operating in the continuous conduction mode. Power stage of figure 4.2, controller of figure 2.2	79
4.13	Output impedance of a constant-frequency current step-up converter operating in the continuous conduction mode. Power stage of figure 4.2, controller of figure 2.2. Output impedance in dB referenced to 1 Ω	81
4.14	Closed-loop gain of a constant frequency current step-up converter operating in the continuous conduction mode. Power stage of figure 4.2, controller of figure 2.2	83
4.15	Audio susceptibility of a constant-frequency current step-up converter operating in the continuous conduction mode. Power stage of figure 4.2, controller of figure 2.2	85
4.16	Loop gain of a constant-frequency current step-up converter operating in the discontinuous conduction mode. Power stage of figure 4.2, controller of figure 2.2	88
4.17	Output impedance of a constant-frequency current step-up converter operating in the discontinuous conduction mode. Power stage of figure 4.2, controller of figure 2.2. Output impedance in dB referenced to 1 Ω	90
4.18	Closed-loop gain of a constant-frequency current step-up converter operating in the discontinuous conduction mode. Power stage of figure 4.2, controller of figure 2.2	92
4.19	Audio susceptibility of a constant-frequency current step-up converter operating in the discontinuous conduction mode. Power stage of figure 4.2, controller of figure 2.2	94

LIST OF TABLES

TABLES		PAGES
4.1	Loop Gain FQVU Mode 1 (Magnitude, Phase)	60
4.2	Output Impedance FQVU Mode 1 (Magnitude)	62
4.3	Closed-Loop Gain FQVU Mode 1 (Magnitude)	64
4.4	Audio Susceptibility FQVU Mode 1 (Magnitude)	66
4.5	Loop Gain FQVU Mode 2 (Magnitude, Phase)	69
4.6	Output Impedance FQVU Mode 2 (Magnitude)	71
4.7	Closed-Loop Gain FQVU Mode 2 (Magnitude)	73
4.8	Audio Susceptibility FQVU Mode 2 (Magnitude)	75
4.9	Loop Gain FQCU Mode 1 (Magnitude and Phase)	78
4.10	Output Impedance FQCU Mode 1 (Magnitude)	80
4.11	Closed-Loop Gain FQCU Mode 1 (Magnitude)	82
4.12	Audio Susceptibility FQCU Mode 1 (Magnitude)	84
4.13	Loop Gain FQCU Mode 2 (Magnitude and Phase)	87
4.14	Output Impedance FQCU Mode 2 (Magnitude)	89
4.15	Closed-Loop Gain FQCU Mode 2 (Magnitude)	91
4.16	Audio Susceptibility FQCU Mode 2 (Magnitude)	93

MEASUREMENT TECHNIQUES FOR THE CHARACTERIZATION IN THE FREQUENCY DOMAIN OF REGULATED ENERGY-STORAGE DC-TO-DC CONVERTERS

CHAPTER I

INTRODUCTION

Reactor energy-storage dc-to-dc converters are presently among the most efficient methodsof dc power conditioning. As a result they are seeing widespread applications wherever dc power is needed. Dc-to-dc converter technology has progressed from the cut-and-try designs of the past to advanced mathematical methods for modeling and design. These highly sophisticated methods are justifiable because of their increasing popularity due to the high efficiency of the system and because the family of energy-storage regulated dc-to-dc converters presents many formidable problems in the design of individual components and of complete systems due to the highly nonlinear characteristics inherent in these converters. One area of paramount concern and, until recently, limited understanding is the predictability of the stability of closed-loop regulated dc-to-dc converters. The lack of analytical methods to study the stability of these systems has caused many users to avoid dc-to-dc switching converters and to opt for less efficient series regulators or other dissipative regulators.

As recently as 1973 [1] small-signal frequency-domain characterization of dc-to-dc converters was introduced. These small-signal models employ various methods to essentially linearize the highly nonlinear dc-to-dc converter about an operating point. This linearization allows the application of familiar linear control theory to the nonlinear system. Loop gain and closed-loop gain can be calculated. Gain margin and phase margin can be obtained from the loop gain of the system and can be used as criteria for the design of a dc-to-dc converter or they can be used to determine the degree

of stability of an existing converter.

In addition to the conventional loop gain and closed-loop gain that provide information about the stability of the isolated converter these small-signal methods can also be used to predict the behavior of a converter in different input and output environments. Input impedance and output impedance can be calculated in the frequency domain allowing the predicting of the effects of an input filter stage or a frequency dependent load on total system stability. Knowledge of the input impedance of a dc-to-dc converter will also allow optimum design of an antecedent input filter stage to ensure total system stability. Another transfer function of interest is the attenuation of a disturbance on the input voltage through the closed loop converter to the output voltage. This transfer function is termed "audio susceptibility" and provides valuable information when comparing the performance of two or more converters.

Many different analytical models are available [1-6], however, to the author's knowledge, there has been very little documentation concerning the physical measurement of these small-signal frequency-domain transfer functions. The existence of these measurements is important for two reasons. First, to verify the validity of the existing models, and second, to allow the characterization in the frequency domain of systems that are too complex to allow exact modeling. This work introduces simple procedures for the measurement of the loop gain, closed-loop gain, output impedance, and the audio susceptibility of closed-loop regulated dc-to-dc converters. Procedures for the measurement of input impedance are not presented in this thesis.

Chapter II includes a brief presentation of one small-signal analytical model of the power stage of a dc-to-dc converter. Also included in Chapter II is the small-signal analysis of a feedback controller network that is used

in conjunction with the power stage to construct a closed-loop converter. The Chapter III presents the procedures of the measurement techniques that are the principal subject of this effort. Finally, in Chapter IV, experimental results are obtained from two experimental converters and are compared with data calculated by computer from the analytical model of the closed-loop system discussed in Chapter II.

CHAPTER II

ANALYTICAL DERIVATION OF CONVERTER SMALL-SIGNAL TRANSFER FUNCTIONS

Power Stage Transfer Functions

Analytical modeling of inductor-energy-storage power stages is a specific application of the linearization of switched networks containing energy storage elements. Many studies have been concerned with the development of small-signal models for converter power stages [1-6]. These studies vary widely in the specific approach to the problem but fortunately they all lead to essentially identical final results.

Almost all of the research efforts in this field have modeled the elements in the power stage as ideal or near-ideal. Capacitor equivalent series resistance (ESR) is often the only loss taken into account. The results of physical measurements presented as a topic for this thesis have demonstrated the need to include additional losses in the power stage elements. As a result, one of the simplified linearization schemes has been modified to include resistive losses in the power stage transistor switch, the commutating diode, and in the windings of the energy-storage-inductor [2]. The admission of these losses in the analysis greatly improves the correlation between analytical results and experimental measurement. The complete derivation of this modified linearization scheme is complex and detailed discussion will not be attempted in this report. Instead a brief overview will be presented to provide continuity.

A model of the voltage step-up power stage network that is used as

an example for this linearization scheme is shown in figure 2.1a. The variational output current i_0 is a current that is injected into the circuit allowing a small signal perturbation for the measurement and calculation of output impedance. The transistor switch and the output diode in the power stage may be represented by the piecewise linear approximations appearing in figure 2.1b. The state variables for this network are the inductor current and capacitor voltage i_x and v_c. Idealized waveforms for these state variables appear in figure 2.1c. The duty cycle (on-time divided by the total switching period) of the power stage transistor switch is determined by a controller that continuously monitors the output voltage of the converter. The analytical derivation of the gain function of the controller will be discussed in the next section.

Referring to figure 2.1c the power stage transistor switch is turned on at $t=t_0$ and off at time $t= \quad t_{on}$ by the duty cycle controller. The transistor switch is turned on again at $t=T+t_0$ where T is the switching period of the controller. If the inductor current should fall to zero during the off time of the transistor the converter is said to be operating in the discontinuous conduction mode. T_{off}' and T_{off}'' indicate the interval where the inductor current is non-zero and zero respectively during the transistor off time. If the inductor current never falls to zero ($T_{off}''=0$) the converter is said to be operating in the continuous conduction mode.

During each of the three different time intervals (T_{on}, T_{off}', T_{off}'') the elements of the converter will appear in three different configurations that may be described by three different sets of state equations. These three different configurations are shown in figure 2.1d. All three sets are needed to describe the converter behavior in the discontinuous conduction

ORIGINAL PAGE IS
OF POOR QUALITY

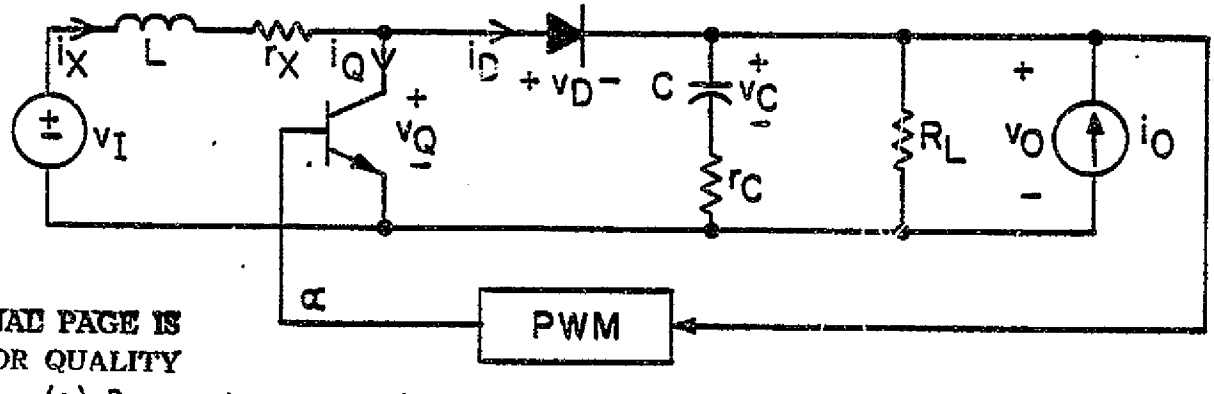

(a) Power stage network model

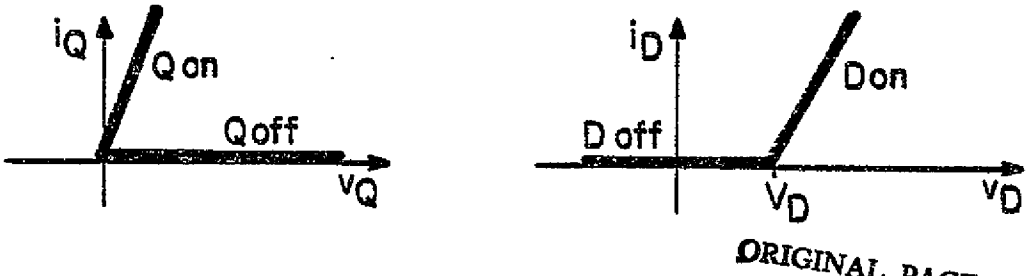

(b) Transistor and diode models

ORIGINAL PAGE IS
OF POOR QUALITY

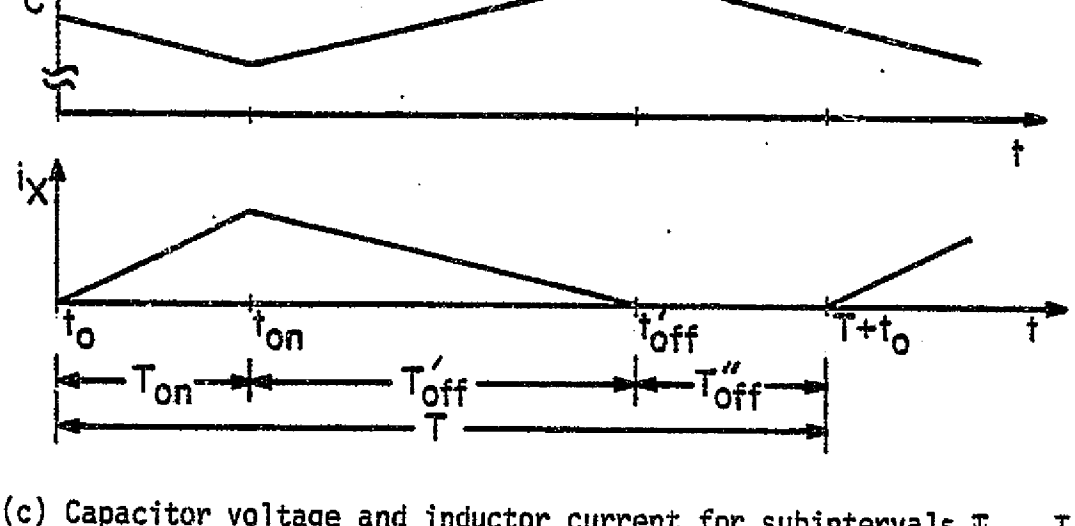

(c) Capacitor voltage and inductor current for subintervals T_{on}, T_{off}', T_{off}''

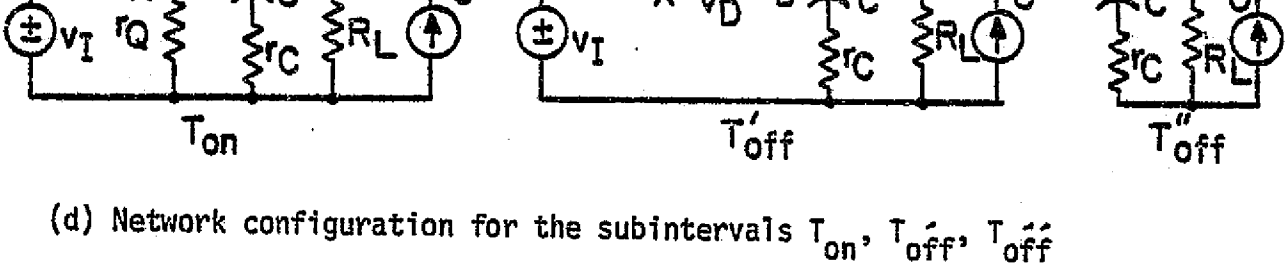

(d) Network configuration for the subintervals T_{on}, T_{off}', T_{off}''

Figure 2.1 Circuit model and state variable waveforms for a small-signal analysis of the constant-frequency voltage step-up converter

mode but only two sets are necessary for the continuous conduction mode ($T_{\tilde{off}} = 0$). The converter performance over the entire switching period T can thus be obtained by applying the appropriate set of state equations during the corresponding time interval. The initial conditions of one set of equations are determined by the values held at the end of the previous time interval (determined by the previous set of state equations).

For simplicity only continuous conduction operation will be described here. Discontinuous conduction analysis is similar but uses an additional set of state equations for the interval $T_{\tilde{off}}$.

During the interval $t_0 \leq t \leq t_{on}$ the power stage transistor is on and the state equations are

$$\frac{dv_C}{dt} = f_1(v_C, i_0) \; ; \; \frac{d^2v_C}{dt^2} = \frac{df_1(\cdot)}{dt}$$

$$\frac{di_X}{dt} = g_1(i_X, v_I) \; ; \; \frac{d^2i_X}{dt^2} = \frac{dg_1(\cdot)}{dt} \qquad (2.1)$$

During the interval $t_{on} \leq t \leq T + t_0$ the power stage transistor is off and the state equations are

$$\frac{dv_C}{dt} = f_2(v_C, i_X, v_I, i_0) \; ; \; \frac{d^2v_C}{dt^2} = \frac{df_2(\cdot)}{dt}$$

$$\frac{di_X}{dt} = g_2(v_C, i_X, v_I, i_0); \; \frac{d^2i_X}{dt^2} = \frac{dg_2(\cdot)}{dt} \qquad (2.2)$$

The state variable waveshapes may be approximated by a Taylor series expansion retaining only the first three terms. The Taylor series is an acceptable method to obtain the solutions for the end of each time interval (t_{on} and t_0+T) in terms of the initial conditions and derivatives at the beginning of each time interval (t_0 and t_{on}). So for the interval beginning at t_0 and ending at t_{on}

$$v_C(t_{on}) = v_C(t_0) + (t_{on}-t_0)\frac{dv_C(t_0)}{dt} + \frac{(t_{on}-t_0)^2}{2!}\frac{d^2v_C(t_0)}{dt^2}$$

$$i_X(t_{on}) = i_X(t_0) + (t_{on}-t_0)\frac{di_X(t_0)}{dt} + \frac{(t_{on}-t_0)^2}{2!}\frac{d^2i_X(t_0)}{dt^2} \qquad (2.3)$$

And for the interval beginning at t_{on} and ending at T

$$v_C(T+t_0) = v_C(t_{on}) + (T+t_0-t_{on})\frac{dv_C(t_{on})}{dt} + \frac{(T+t_0-t_{on})^2}{2!}\frac{d^2v_C(t_{on})}{dt^2}$$

$$i_X(T+t_0) = i_X(t_{on}) + (T+t_0-t_{on})\frac{di_X(t_{on})}{dt} + \frac{(T+t_0-t_{on})^2}{2!}\frac{d^2i_X(t_{on})}{dt^2} \qquad (2.4)$$

Combining 2.1 and 2.3 and setting t_0 to 0 (t_0 being an arbitrary starting time) and replacing $(t_{on}-t_0)$ with T_{on}.

$$v_C(t_{on}) = v_C(0) + T_{on}f_1(v_C,i_0) + \frac{T_{on}^2}{2!}\frac{df_1(\cdot)}{dt}$$

$$i_X(t_{on}) = i_X(0) + T_{on}g_1(i_X,v_I) + \frac{T_{on}^2}{2!}\frac{dg_1(\cdot)}{dt} \qquad (2.5)$$

combining 2.2 and 2.4 and replacing $(T+t_o-t_{on})$ with T_{off}

$$v_C(T) = v_C(t_{on}) + T'_{off} f_2(v_C, i_X, v_I, i_O) + \frac{T'^2_{off}}{2!} \frac{df_2(\cdot)}{dt}$$

$$i_X(T) = i_X(t_{on}) + T'_{off} g_2(v_C, i_X, v_I, i_O) + \frac{T'^2_{off}}{2!} \frac{dg_2(\cdot)}{dt} \qquad (2.6)$$

Substituting 2.5 into 2.6

$$v_C(T) = v_C(0) + T_{on} f_1(v_C, i_O) + T'_{off} f_2(v_C, i_X, v_I, i_O) + \frac{T_{on}^2}{2!} \frac{df_1(\cdot)}{dt} + \frac{T'^2_{off}}{2!} \frac{df_2(\cdot)}{dt}$$

$$i_X(T) = i_X(0) + T_{on} g_1(i_X, v_I) + T'_{off} g_2(v_C, i_X, v_I, i_O) + \frac{T_{on}^2}{2!} \frac{dg_1(\cdot)}{dt} + \frac{T'^2_{off}}{2!} \frac{dg_2(\cdot)}{dt} \qquad (2.7)$$

Equations 2.7 are known as discrete-time-recursion equations for recursion period T. These equations describe the performance of the dc-to-dc converter at the end of the switching cycle by using information available at the beginning of each switching cycle. Description of the operation of the system at intermediate values of time during the period T has been obscured. Rearranging equations 2.7 and dividing each side by T results in

$$\frac{v_C(T) - v_C(0)}{T} = \frac{T_{on}}{T} f_1(v_C, i_O) + \frac{T'_{off}}{T} f_2(v_C, i_X, v_I, i_O) + \frac{T_{on}^2}{2T} \frac{df_1(\cdot)}{dt} + \frac{T'^2_{off}}{2T} \frac{df_2(\cdot)}{dt}$$

$$\frac{i_X(T) - i_X(0)}{T} = \frac{T_{on}}{T} g_1(i_X, v_I) + \frac{T'_{off}}{T} g_2(v_C, i_X, v_I, i_O) + \frac{T_{on}^2}{2T} \frac{dg_1(\cdot)}{dt} + \frac{T'^2_{off}}{2T} \frac{dg_2(\cdot)}{dt} \qquad (2.8)$$

Equations 2.8 are discrete-time difference equations for the difference period T, divided by the period T. If the time variables are assumed to change only slowly with respect to the total switching period, equations 2.8 can be written in the form of differential equations. For this reason

this small signal model is valid only for frequencies up to half of the converter switching frequency. The value of a physical measurement beyond half of the conversion frequency is also questionable so no problem arises from this limitation on the model. Rewriting equations 2.8 in the form of differential equations and replacing (T_{on}/T) with the duty ratio α and (T_{off}/T) with $(1-\alpha)$ provides

$$\frac{dv_C^*}{dt} = \alpha f_1(v_C^*, i_0) + (1-\alpha) f_2(v_C^*, i_X^*, v_I, i_0) + \frac{T}{2}\alpha^2 \frac{df_1(\cdot)}{dt} + \frac{T}{2}(1-\alpha)^2 \frac{df_2(\cdot)}{dt}$$

$$= f_{v_C^*}(v_C^*, i_X^*, \alpha, v_I, i_0)$$

$$\frac{di_X^*}{dt} = \alpha g_1(i_X^*, v_I) + (1-\alpha) g_2(v_C^*, i_X^*, v_I, i_0) + \frac{T}{2}\alpha^2 \frac{dg_1(\cdot)}{dt} + \frac{T}{2}(1-\alpha)^2 \frac{dg_2(\cdot)}{dt} \qquad (2.9)$$

$$= f_{i_X^*}(v_C^*, i_X^*, \alpha, v_I, i_0)$$

v_C^* and i_I^* in equations 2.9 are distinct from v_C and i_X in all previous equations because equations 2.9 are continuous-time differential equations that have been derived from discrete-time equations concerned only with the behavior of the converter at exact points in time (t_0 and t_0+T). Equations 2.9 provide no information concerning the behavior of the converter between these points in time. However, if small signal variations are the only concern, equations 2.9 prove very useful.

If the variables in the right-hand side of equations 2.9 are allowed to have variational (ac) components then equations 2.9 can be rewritten

$$\frac{dv^*_{C,ac}}{dt} = a_{11}v^*_{C,ac} + a_{12}i^*_{X,ac} + b_{11}\alpha_{ac} + b_{12}v_{I,ac} + b_{13}i_{0,ac}$$

$$\frac{di^*_{X,ac}}{dt} = a_{21}v^*_{C,ac} + a_{22}i^*_{X,ac} + b_{21}\alpha_{ac} + b_{22}v_{I,ac} + b_{23}i_{0,ac} \qquad (2.10)$$

where:

$$a_{11} = \frac{\partial f_{v^*_C}}{\partial v^*_C}$$

$$a_{12} = \frac{\partial f_{v^*_C}}{\partial i^*_X}$$

$$b_{11} = \frac{\partial f_{v^*_C}}{\partial \alpha}$$

$$b_{12} = \frac{\partial f_{v^*_C}}{\partial v_I}$$

$$b_{13} = \frac{\partial f_{v^*_C}}{\partial i_0}$$

and:

$$a_{21} = \frac{\partial f_{i^*_X}}{\partial v^*_C}$$

$$a_{22} = \frac{\partial f_{i^*_X}}{\partial i^*_X}$$

$$b_{21} = \frac{\partial f_{i^*_X}}{\partial \alpha}$$

$$b_{22} = \frac{\partial f_{i^*_X}}{\partial v_I}$$

$$b_{23} = \frac{\partial f_{i^*_X}}{\partial i_0}$$

The derivation is now at the point of making the final step in the small-signal analysis of the voltage step-up power stage. Transformation of the time differential equations in 2.10 into the frequency domain is accomplished by applying the Laplace transform assuming that the system is initially at rest with the initial conditions of all perturbations equal to zero. The results of the transform are

$$sV_C(s) = a_{11}V_C(s) + a_{12}I_X(s) + b_{11}A(s) + b_{12}V_I(s) + b_{13}I_0(s)$$

$$sI_X(s) = a_{21}V_C(s) + a_{22}I_X(s) + b_{21}A(s) + b_{22}V_I(s) + b_{23}I_0(s) \qquad (2.11)$$

Equations 2.11 can be rearranged and combined to obtain $V_C(s)$ and $I_X(s)$ in terms of $A(s)$, $V_I(s)$ and $I_0(s)$. Further manipulations will provide these dependences with gain constants, zeroes and poles.

The most important concern in converter systems is the output voltage $v_0(t)$ and its transformed counterpart $V_0(s)$. By using the value of the filter capacitor and the value of the equivalent series resistance of the filter capacitor, it is possible to determine $v_0(t)$ in terms of $v_C(t)$ and similarly $V_0(s)$ in terms of $V_C(s)$.

The frequency dependent transfer functions of concern are audio susceptibility $V_0(s)/V_I(s)$, and output impedance $V_0(s)/I_0(s)$. For the case of the voltage step-up converter dynamic input impedance is available from the ratio $V_I(s)/I_X(s)$. The duty cycle controller provides the transfer ratio $A(s)/V_0(s)$. Utilizing the duty-cycle transfer ratio with the power stage transfer ratio allows the calculation of loop gain and closed-loop gain.

Similar reasoning can be applied to the current step-up and the current-or-voltage step-up dc-to-dc converters to obtain frequency domain models. It should be noted that the steps involved in modeling the converters without the all important losses are identical to the analytical procedure outlined here. The lossy case is more complex but is also more descriptive of the physical circuit.

Feedback Controller Transfer Functions

The gain of the composite feedback controller network may be evaluated by separating the network into three cascaded gains. The first gain is β the resistive attenuator gain. The second gain is that of the error amplifier. The final stage of the feedback network is the pulse width modulator (PWM). The PWM is actually an analog to pulse-train converter producing an output pulse with a width that is proportional to the input voltage. This proportionality is the gain of the PWM stage. The circuit diagram of the feedback controller network is shown in figure 2.2.

The resistive attenuator gain may be obtained by a simple voltage divider calculation. Including the input impedance of the error amplifier, the resistive divider appears as in figure 2.3. The exact values of R_1 and R_2 depend on the level of output voltage. Two power stages are used in the Chapter IV to compare theory and experiment. These power stages are a voltage step-up and a current step-up converter. They both use the same feedback controller network but operate with different output voltages and therefore with different values of β.

For the voltage step-up converter

$V_0 = 28V$ $R_1 = 15k\Omega$ $R_2 = 4k\Omega$

$\beta = 0.16$

For the current step-up converter

$V_0 = 12V$ $R_1 = 8.2k\Omega$ $R_2 = 10.8k\Omega$

$\beta = 0.39$

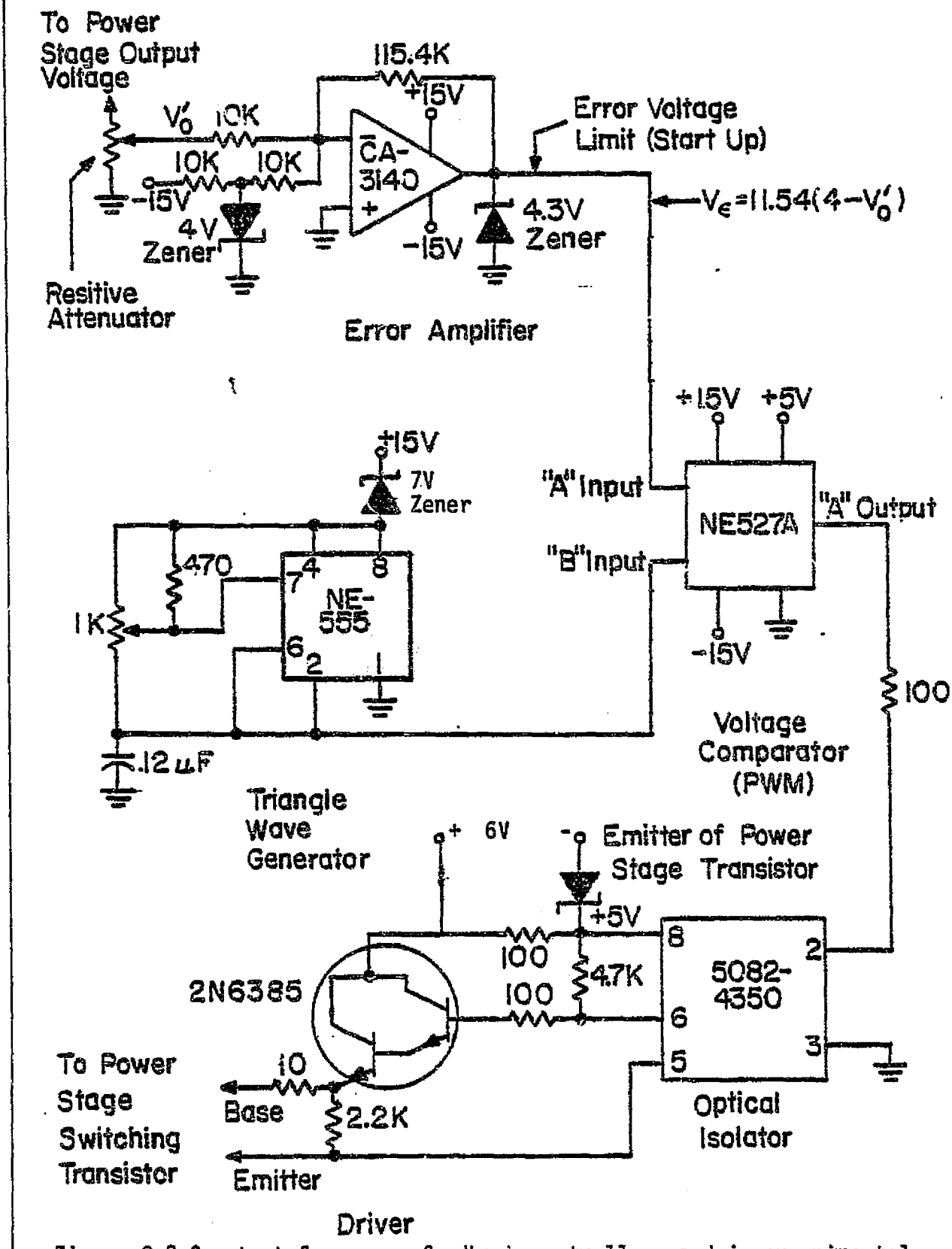

Figure 2.2 Constant-frequency feedback controller used in experimental converters of chapter IV.

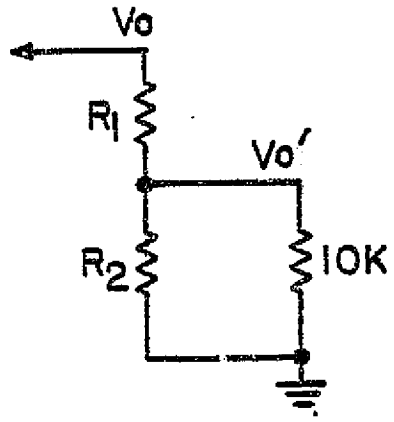

Figure 2.3 Resistive attenuator network of figure 2.2

$$\frac{V_o'}{V_o} = \frac{R_2 \,||\, 10k\Omega}{R_2 \,||\, 10k\Omega + R_1} = \beta$$

ORIGINAL PAGE IS
OF POOR QUALITY

The next stage is the error amplifier. This particular error amplifier is an operational amplifier in an inverting summer configuration. The reference voltage is negative providing a difference amplifier operation. The isolated error amplifier and the corresponding gain calculations appear in figure 2.4. The constant K may be disregarded because only small signal changes are of concern.

The error voltage limit Zener diode shown in figure 2.2 is not involved in the evaluation because the Zener effect is only present during start-up and some transients. The diode appears as an open circuit during steady-state operation. The Zener diode is present to ensure a maximum on-time for the power stage switching transistor.

The PWM gain can be determined graphically. A straight-line approximation of the triangle generator output is shown in figure 2.5. Using a straight-line approximation instead of the true exponential capacitor charging voltage is justified because only small signal perturbations are of concern. An oscillogram of the actual triangle waveshape is shown in figure 2.6.

Figure 2.5 illustrates the action of the voltage comparator by superimposing an arbitrary error voltage of 4 volts on top of the triangle generator output. The corresponding on-time and off-time are indicated below the time axis. An oscillogram of this operation is shown in figure 2.7. The discontinuities in the error voltage in figure 2.7 are due to the equivalent series resistance of the power stage output filter capacitor. A slight delay can be seen between the crossing of the two voltage waveforms and the turn on/off of the power transistor base drive. These delays are constant for any value of duty cycle and therefore have limited effect on small signal gain calculations.

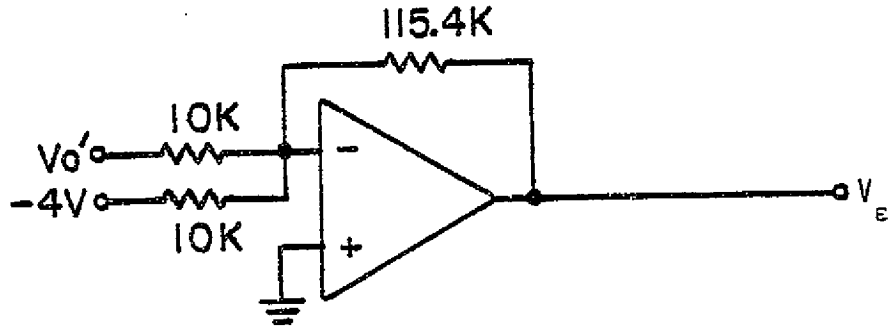

Figure 2.4 Error amplifier network of figure 2.2

$$V_\varepsilon = \frac{115.4}{10}(4-V_o')$$

$$= K - 11.54V_o'$$

$$\frac{\partial V_\varepsilon}{\partial V_o'} = \frac{\Delta V_\varepsilon}{\Delta V_o'} = 11.54$$

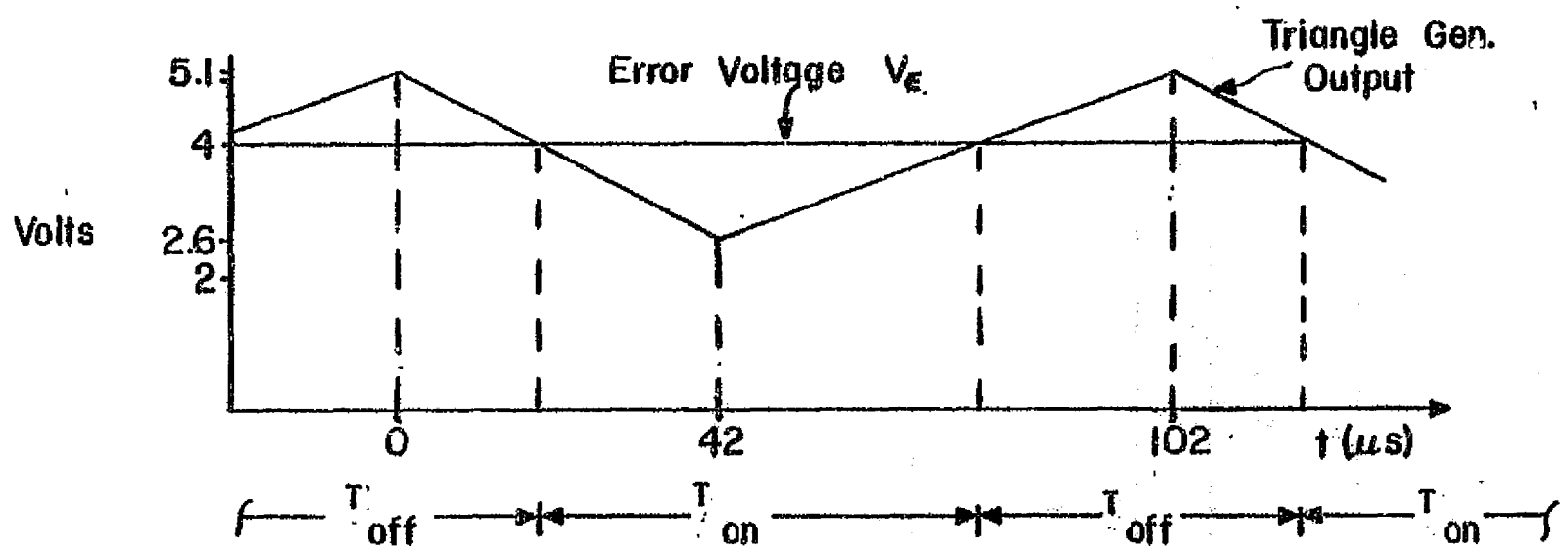

Figure 2.5 Straight line approximation of triangle wave generator of figure 2.2 with an arbitrary error voltage of 4.0 Volts. Corresponding on-time and off-time indicated below.

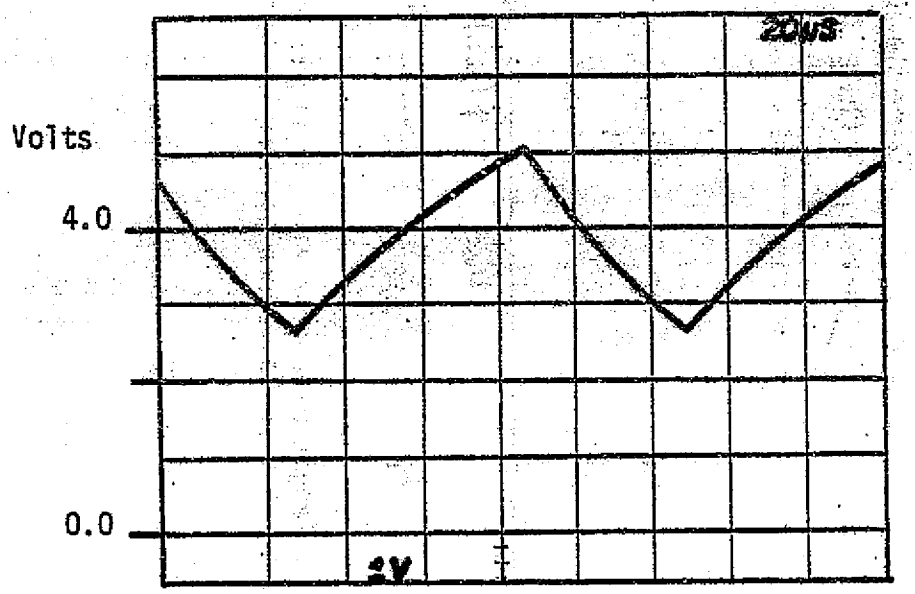

Figure 2.6 Oscillogram of the output of the triangle wave generator taken from the circuit of figure 2.2

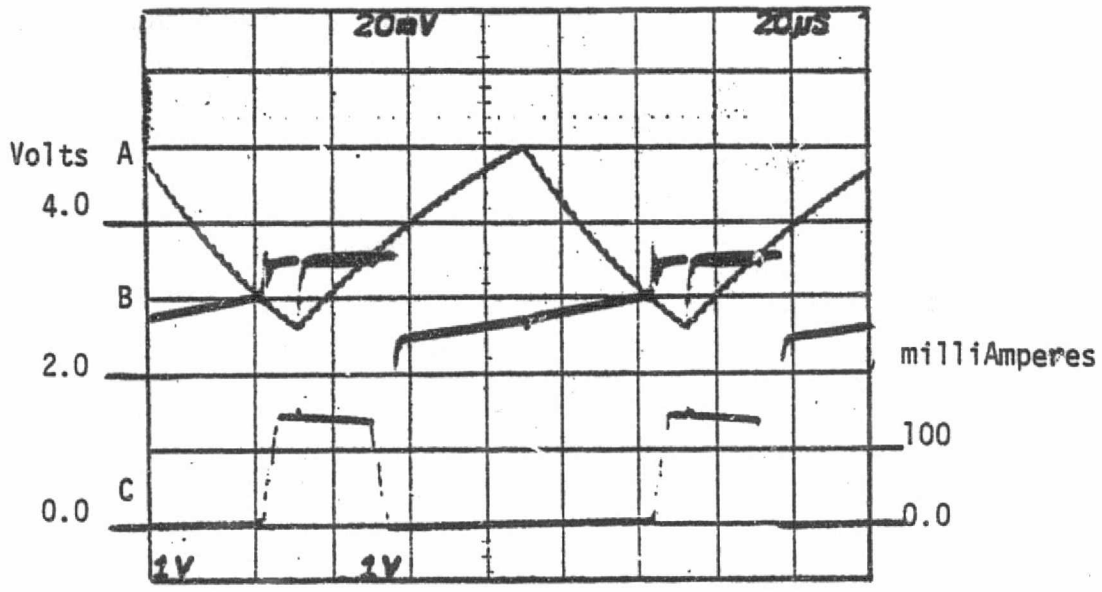

Figure 2.7 Oscillogram of the triangle wave generator and error voltage with the corresponding base drive on-time and off-time indicated below. Oscillogram taken from circuit of figure 2.2.A: Triangle wave generator, B: Error voltage C:Base drive current

PWM gain calculations can be obtained by dividing the stragith line triangle wave approximation into two ramp-like waves. Each ramp will control the gain along one edge of the total on-time pulse. Figure 2.8 illustrates this idea.

$$T_{on_1} = \frac{(V_\varepsilon - V_b)T_1}{V_a - V_b}$$

$$T_{on_2} = \frac{(V_\varepsilon - V_b)T_2}{V_a - V_b}$$

$$T_{on} = T_{on_1} + T_{on_2} = \frac{(V_\varepsilon - V_b)(T_1 + T_2)}{V_a - V_b}$$

$$= \frac{(V_\varepsilon - V_b)T}{V_a - V_b}$$

$$\alpha = \frac{T_{on}}{T} = \frac{V_\varepsilon - V_b}{V_a - V_b}$$

$$\frac{\partial \alpha}{\partial V_\varepsilon} = \frac{\Delta \alpha}{\Delta V_\varepsilon} = \frac{1}{V_a - V_b}$$

For the constant-frequency controller being analyzed

$$V_a = 5.1V \qquad V_b = 2.6V$$

$$\frac{\Delta \alpha}{\Delta V_\varepsilon} = \frac{1}{(5.1 - 2.6)} = .4$$

This result may also be intuitively realized by observing that varying α from 0 to 1.0 requires an error voltage swing from 2.6 to 5.1 volts.

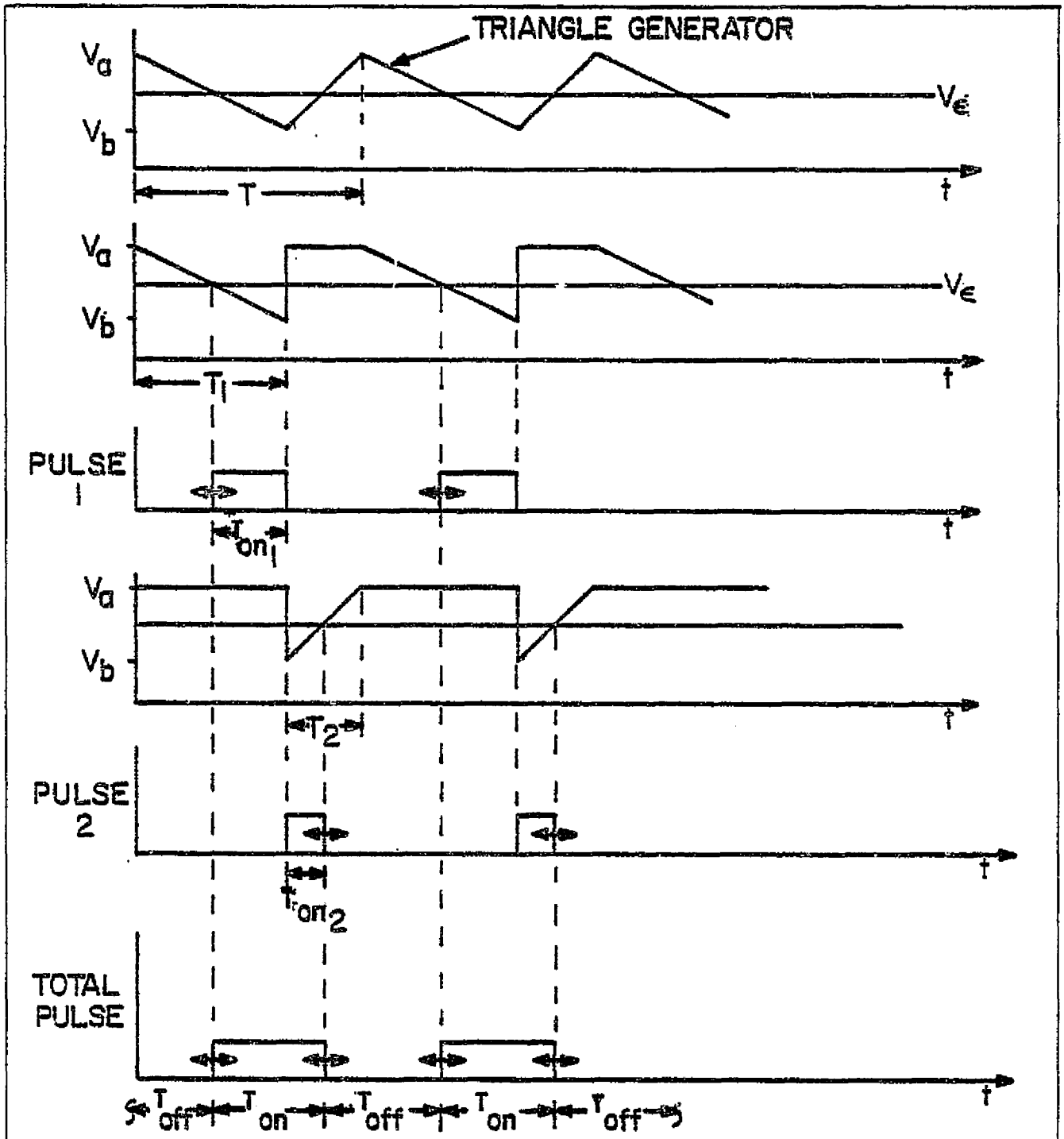

Figure 2.8 Time graphs for the derivation of the gain of the pulse-width-modulator of the circuit of figure 2.2.

$$\frac{\Delta\alpha}{\Delta V_\varepsilon} = \frac{1-0}{5.1-2.6} = .4$$

As mentioned before, the composite gain of the feedback loop can be evaluated by cascading the three gains that have been determined.

$$\frac{\Delta\alpha}{\Delta V_0} = \frac{\Delta V_0'}{\Delta V_0} \times \frac{\Delta V_\varepsilon}{\Delta V_0'} \times \frac{\Delta\alpha}{\Delta V_\varepsilon}$$

$$= \beta\ (11.5)(.4) = 4.6\beta = A(s)/V_0(s)$$

The gain is determined assuming that there are no frequency dependent elements present in the feedback loop. This is a realistic assumption if the small signal sinusoidal perturbation frequency is small with respect to the bandwidth of the error amplifier.

For the voltage step-up converter with $\beta = 0.16$

$$A(s)/V_0(s) = 0.53$$

For the current step-up converter with $\beta = 0.39$

$$A(s)/V_0(s) = 1.8$$

In chapter IV the quantity $A(s)/V_0(s)$ is entered into a computer analysis program as βH_F where $H_F = 4.6$ and β is the appropriate value corresponding to the power-stage under analysis.

CHAPTER III

EXPERIMENTAL MEASUREMENT PROCEDURES

Introduction

In this chapter experimental procedures are presented for the measurement of four important frequency-domain transfer functions of closed-loop regulated dc-to-dc converters. The four transfer functions are; loop gain, output impedance, closed-loop gain, and audio susceptibility. Each procedure is preceded by a diagram of the experimental layout. It is strongly suggested that before using any of the procedures the experimentor should thoroughly read and understand the necessary steps involved.

An equipment list is included as the first section of each procedure. This equipment list is not intended to be restrictive as equipment substitutions are of course possible. The procedures are by no means unique. They are but one way of obtaining valid experimental data. Any constructive innovation by the reader is encouraged.

All four of the measurement schemes use a wave analyzer as the basic measurement tool. A wave analyzer contains a frequency tunable voltmeter that will provide only RMS magnitude information. For this reason only the magnitude of the transfer function is accessible for all of the transfer functions except loop gain where both magnitude and phase are available.

All of the measurement procedures involve the injection of a small perturbation voltage into the closed-loop converter system. This voltage injection is accomplished by using an audio isolation transformer manufactured

by Solar Electronics. This transformer is an energy-storage transformer that is specifically designed to allow the injection of small-signal perturbations into conductors carrying large dc currents.

Each of the procedures recuire the measurement of small sinusoidal perturbation voltages riding on a dc level. Following accepted convention, these small-signal perturbational components of the entire signal are labeled with a capital primary letter subscripted by a lower-case letter followed by a lower-case "e" to indicate the RMS value of the small-signal sinusoidal voltage. As an example the symbol "V_{ie}" represents the RMS magnitude of the perturbation voltage at the input of the dc-to-dc converter. The fact that the RMS magnitude is indicated is because it is this magnitude that is provided by this particular voltmeter. The peak-to-peak or zero-to-peak magnitude can also be used because the magnitudes of the small-signal perturbations always appear in ratios with voltage magnitudes in both the numerator and denominator.

The measurement of loop gain is obtained from a procedure outlined by B.D. Pierce [7] intended for use in feedback systems containing integrators and later expanded by R.D. Middlebrook [8] to an application to dc-to-dc converters. A closed-loop dc-to-dc converter is similar to a feedback system containing integrators because if the loop is opened to facilitate the measurement of loop gain, the operating point of the system is destroyed making any measurements ambiguous. For this reason it is necessary to measure loop gain while the system is operating closed-loop. This is accomplished by injecting a voltage with the audio isolation transformer at a point in the loop such that the impedance to ground in the forward direction around the loop is much greater than the impedance to ground

looking backward around the loop. Such a point is available in all dc-to-dc converters between the load and the resistive attenuator of the controller network. There are thus three voltages available. These voltages are shown in figure 3.2 as v_x, v_y, and v_z and are related such that $v_z = v_x + v_y$. The magnitude of the transfer function is the ratio of V_{ye} to V_{xe} and by using the magnitude of the injected voltage V_{ze} phase information is obtainable.

$$\text{Loop Gain} = 20 \log \left(\frac{V_{ye}}{V_{xe}} \right) \text{ dB}$$

$$\angle \pm 2\cos^{-1} \left[\frac{V_{ze}^2 - (V_{xe} - V_{ye})^2}{4 V_{xe} V_{ye}} \right]^{1/2}$$

The sign of the phase of the transfer function is ambiguous but proper choice is usually obvious from the behavior of the magnitude response.

The output impedance of a converter is also measured by a voltage injection method using the isolation transformer. The derivation of the output impedance from a voltage injection is shown below figure 3.1. The output impedance is calculated in decibels referenced to 1Ω to facilitate the display of the data.

$$\text{Output Impedance} = 20 \log \left(\frac{R_L V_{oe}}{V_{oe} - V_{oe}} \right) \text{ dB}$$

The closed-loop gain of a dc-to-dc converter is the susceptibility of the output voltage to a disturbance in the reference voltage. To make comparison between two converters operating at different output voltage

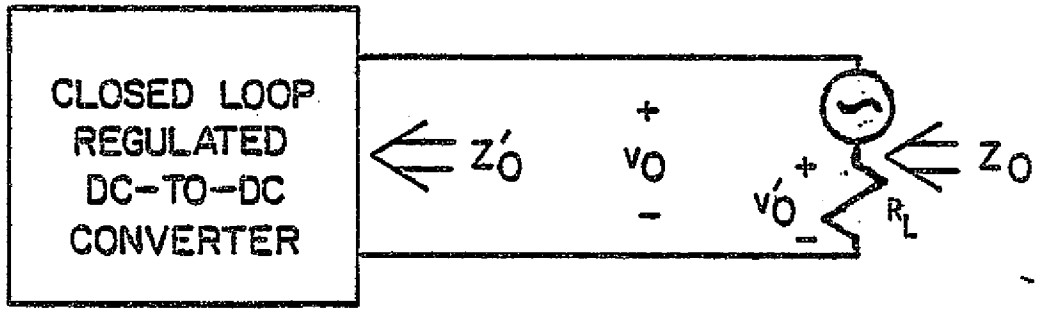

Figure 3.1 Diagram for the derivation of the output impedance of a regulated dc-to-dc converter.

$$\frac{V_{oe}}{Z'_O} = \frac{V'_{oe}}{R_L}$$

$$Z'_O = \frac{V_{oe}}{V'_{oe}} R_L$$

$$Z_O \equiv Z'_O || R_L = \frac{\frac{V_{oe}}{V'_{oe}} R_L^2}{\frac{V_{oe} R_L}{V'_{oe}} + R_L} = \frac{V_{oe} R_L}{V'_{oe} + V_{oe}}$$

and/or reference voltage levels more meaningful, the closed-loop gain presented here is a normalized closed-loop gain.

$$\text{Normalized Closed-Loop Gain} = 20 \log \left(\frac{V_{oe}/V_{O,AVE}}{V_{refe}/V_{REF,AVE}} \right) \text{dB}$$

Audio susceptibility is defined as the susceptibility of the output voltage to disturbances in the input voltage. This transfer function is also normalized to allow comparisons between converters operating at different voltage levels.

$$\text{Audio Susceptibility} = 20 \log \left(\frac{V_{oe}/V_{O,AVE}}{V_{ie}/V_{I,AVE}} \right) \text{dB}$$

The magnitude of the injected voltage used in each of these frequency-domain energy-storage converter measurements is critical. One must remember that these systems are highly nonlinear and too large an injected voltage would make a linear system approximation about an operating point invalid and would lead to distortion in a measured transfer function. The injected voltage should be small enough to preserve a linear system approximation about the operating point but should be large enough to avoid problems due to the unavoidable switching noise present in all converters of this type.

All energy-storage dc-to-dc converters operating at steady-state have two possible modes of operation with respect to the current in the energy storage inductor. If the current through the inductor is not allowed to fall to zero during the switching cycle the converter is said to be operating in the continuous conduction mode, mode 1. If this current is allowed to fall to zero the converter is said to be in mode 2, the

discontinuous conduction mode. The frequency responses of the power stage transfer functions vary vastly from one mode of operation to the other. Precautions are included in all four procedures to ensure that the injected perturbation voltage does not force the converter into both modes of operation during a measurement. If the operating point of the converter is very close to the transition from continuous to discontinuous conduction it may be impossible to find a perturbation voltage small enough to avoid two-mode operation resulting in a false measurement. If this is the case it is suggested that the converter be forced further into the desired mode of operation by an appropriate change in load and that the transfer functions obtained at this new operating point be used as an approximation to those of the desired operating point.

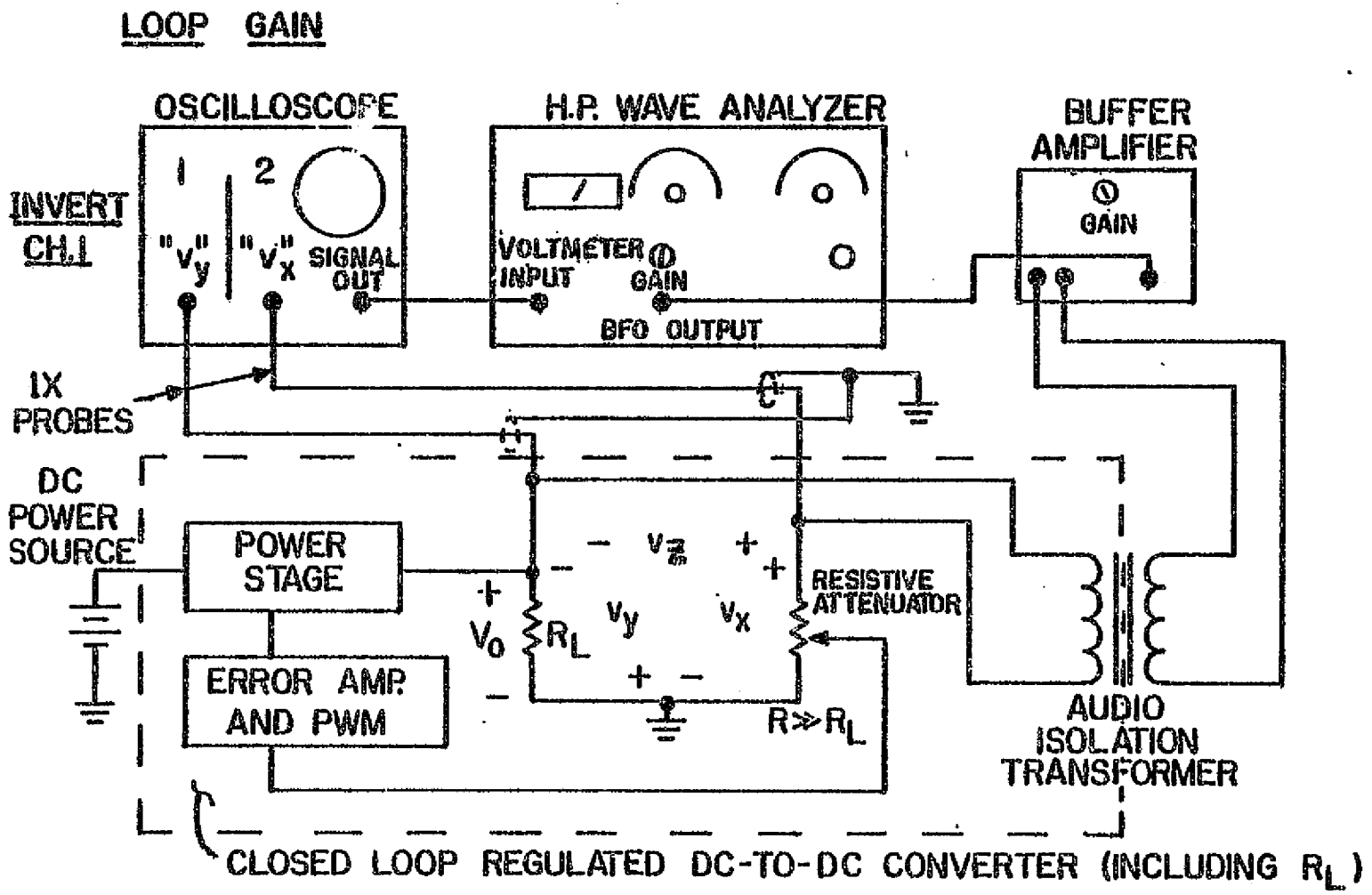

Figure 3.2 Layout diagram for the measurement of loop gain.

Loop Gain [7,8] Reference firgure 3.2

Equipment

DC power source

2 (or more) channel oscilloscope with adding capabilities

Wave analyzer (HP 302A or similar)

2 1x Voltage Probes

Audio isolation transformer (Solar Electronics 6220-1A or similar)

Buffer amplifier (McIntosh 75 or similar)

1 Current probe

Load resistor

Procedure

1) Turn all power off.
2) Place the secondary of the audio isolation transformer between the positive side of the load resistor and the resistive divider network of the controller.
3) Connect the output of the beat frequency oscillator (BFO) in the wave analyzer to the input of the buffer amplifier. Turn the gain of the BFO and the gain of the buffer amplifier to zero (full CCW). Do not connect the output of the buffer amplifier to the isolation transformer.
4) Connect the signal-out (or vertical out) of the oscilloscope to the input of the frequency selective voltmeter in the wave analyzer. Turn the sensitivity of the voltmeter to the least sensitive position.
5) Place a 1x probe on the terminal of the secondary of the audio isolation transformer that is closest to the load resistor (V_{ye}) and connect this probe to channel 1 of the oscilloscope. Invert channel 1 of the

oscilloscope. Place a different 1x voltage probe on the terminal of the audio isolation transformer that is closest to the resistive divider network of the controller (V_{xe}). Connect this probe to channel 2 of the oscilloscope. AC couple both inputs. Set the gain of both channels to 0.1 - 0.2 V/div. The gains must be equal because the oscilloscope will be used in the adding mode. For loop gain tests, the oscilloscope is used as a switch to choose between V_{xe} or V_{ye} and as an adder to add V_{xe} and V_{ye} to obtain V_{ze}.

6) Turn the converter on.

7) Turn on the oscilloscope, wave analyzer, and buffer amplifier.

8) Connect the output of the buffer amplifier to the primary of the audio isolation transformer. This is done after the converter is started to avoid destructive transients passing backward through the isolation transformer and into the output of the buffer amplifier. Warning - If the converter must be shut down, disconnect the buffer amplifier from the audio isolation transformer before restarting.

9) Check the setup by placing the BFO frequency to 30 or 40 hz. Increase the gain of the buffer amplifier and the BFO until a sinusoid appears on the oscilloscope when the two channels are added ($V_{ze} = V_{xe} + V_{ye}$). The magnitude of the injected sinusoid (indicated by the wave analyzer voltmeter) should vary directly with the amplitude of the BFO. If this is not the case repeat all steps.

10) Zero the BFO by placing the frequency at zero and increasing the gains of the BFO and buffer amplifier slightly. Monitor the sum of the two oscilloscope channels (V_{ze}). If the BFO is zeroed properly no sinusoidal oscillations will appear in the oscilloscope voltage waveform. If oscillations are present, adjust the zero set knob

located below the BFO motor drive until the oscilloscope voltage waveform is quiet.

11) The proper magnitude of the injected voltage (V_{ze}) must be chosen. Observe the sum of the two oscilloscope channels (V_{ze}). Place a current probe on the power stage inductor current (I_x). It is desired to observe both V_{ze} and I_x at several points over the frequency range of desired measurement. If more than two channels are available simply connect the current probe to an unused channel. If a two channel oscilloscope is being used either V_{xe} or V_{ye} must be disconnected to allow the observation of I_x.

12) Keeping the magnitude of injected voltage (V_{ze}) constant (magnitude of injected voltage indicated by the voltmeter of the wave analyzer), vary the frequency of the BFO over the range of desired measurement. If the power stage inductor current demonstrates that the converter is moving in and out of both modes of operation (continuous and discontinuous conduction), decrease the magnitude of the BFO. Find a BFO amplitude such that for any frequency the converter is always operating in the desired mode.

    Injected voltage (V_{ze}) may vary with frequency so care must be taken to ensure a constant magnitude for all frequency.

13) It is suggested that the injected voltage to be used for the measurement be no more than 80% of the maximum magnitude determined in the previous step.

    It should be noted that a smaller injected sinusoid will provide results that are more valid than a larger injected sinusoid. The injected voltage should be small to preserve a linear system approximation about the operating point, however, it should be large enough to avoid

problems with switching noise. A typical acceptable injected voltage for loop gain tests would be 50-200 mV RMS.

14) If a two channel oscilloscope is being used remove the current probe from the oscilloscope and replace it with the displaced 1x voltage probe. Check that the gains of the two channels are equal and that channel 1 (V_{ye}) is inverted.

15) Place the BFO at the minimum of the desired frequency range. Adjust and record the magnitude of the small signal injected voltage V_{ze} (determined in steps 12, 13). Record the magnitude of V_{ye} (Channel 1). Record the magnitude of V_{xe} (Channel 2).

16) Adjust the frequency of the BFO to the next point of measurement. Adjust the magnitude of injected voltage ($V_{ze} = V_{xe} + V_{ye}$) until it is the same as that determined in steps 12, 13. Record the magnitude of V_{ye}. Record the magnitude of V_{xe}.

17) Repeat step 16 until the measurement range is covered. 10-15 data points/decade are suggested with at least half in the first two major divisions.

Evaluation

$$\text{Loop Gain} = 20 \log \left(\frac{V_{ye}}{V_{xe}}\right) \text{ dB}$$

$$\angle \pm 2 \cos^{-1} \left[\frac{V_{ze}^2 - (V_{xe} - V_{ye})^2}{4 V_{xe} V_{ye}} \right]^{1/2}$$

Although the sign of the angle of the transfer function is ambiguous, proper choice is usually obvious from the behavior of the magnitude response.

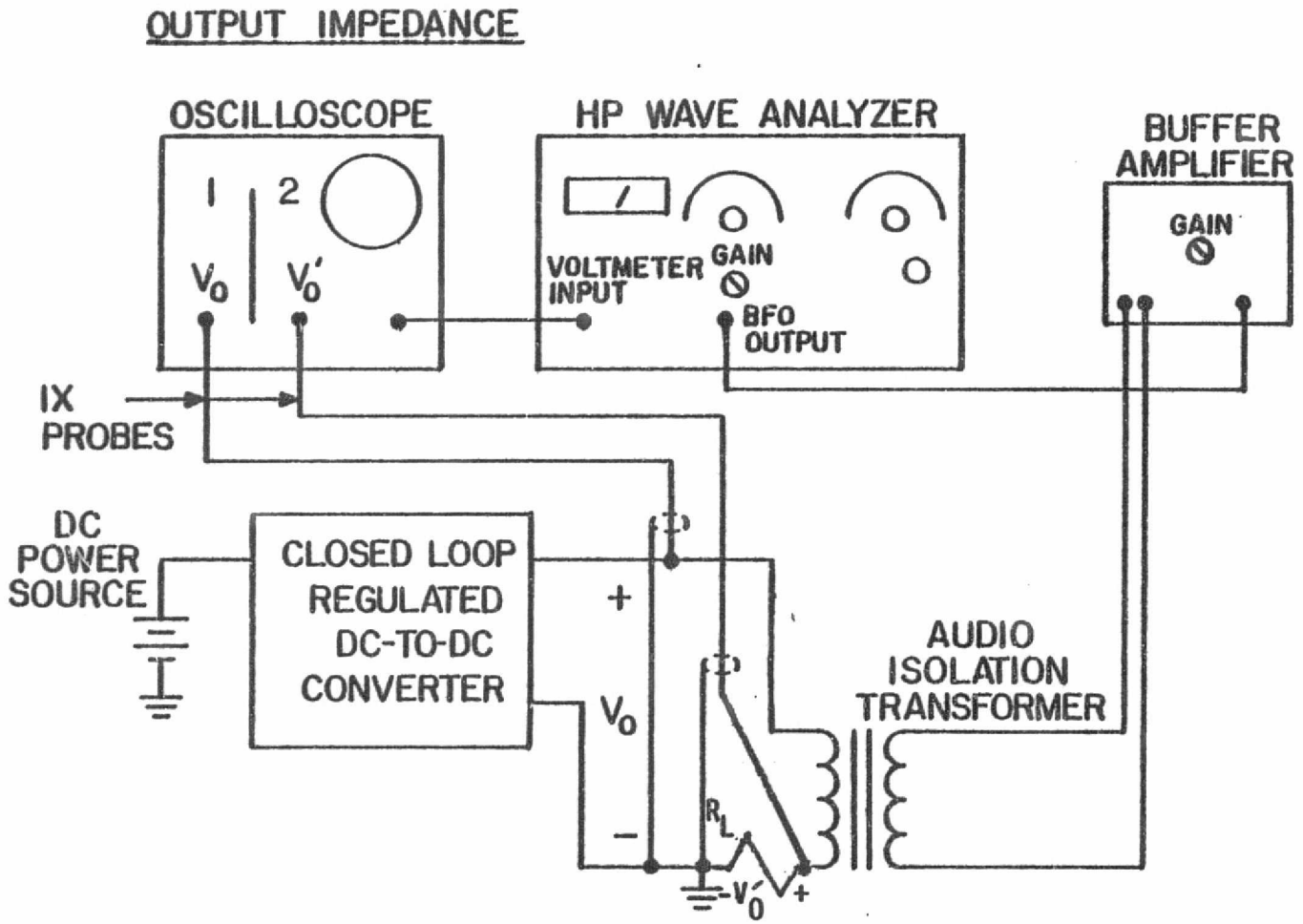

Figure 3.3 Layout diagram for the measurement of output impedance

Output Impedance Reference figure 3.3

Equipment List

DC power source

2 (or more) channel oscilloscope

wave analyzer (HP 302A or similar)

2 1x voltage probes

Audio isolation transformer (Solar Electronics 6220-1A or similar)

Buffer amplifier (McIntosh 75 or similar)

1 Current probe

load resistor

Procedure

1) Turn all power off.

2) Place the secondary of the audio isolation transformer in series with the load resistor between the load resistor and converter positive output.

3) Connect the output of the beat frequency oscillator (BFO) in the wave analyzer to the input of the buffer amplifier. Turn the gain of the BFO and the gain of the buffer amplifier to zero (full CCW). Do not connect the output of the buffer amplifier to the isolation transformer.

4) Connect the signal-out (or vertical out) of the oscilloscope to the input of the frequency selective voltmeter in the wave analyzer. Turn the sensitivity of the voltmeter to the least sensitive position.

5) Place a 1x voltage probe on the output voltage of the dc-to-dc converter (V_{oe}) and connect this probe to channel 1 of the oscilloscope. Place a different 1x voltage probe across the load resistor (V'_{oe}) and connect this probe to channel 2 of the

oscilloscope. AC couple both inputs. Set the gain of both channels to 0.2-0.5V/div(gains should be equal for easier computation). For output impedance tests, the oscilloscope is used only as a switch to choose between channel 1 (V_{oe}) or channel 2 (V'_{oe}).

6) Turn the converter on.

7) Turn on the oscilloscope, wave analyzer and buffer amplifier.

8) Connect the output of the buffer amplifier to the primary of the audio isolation transformer. This is done after the converter is started to avoid destructive transients passing backward through the isolation transformer and into the output of the buffer amplifier. Warning - If the converter must be shut down, disconnect the buffer amplifier from the audio isolation transformer before restarting.

9) Check the setup by placing the BFO frequency to 30 or 40 Hz. Increase the gain of the buffer amplifier and the BFO until motion is present in the voltage waveforms observed on Channel 1 or 2 of the oscilloscope. The magnitude of both waveforms (indicated by the wave analyzer voltmeter) should vary directly with the amplitude of the BFO. If one or both of these tests fails repeat all steps.

10) Zero the BFO by placing the frequency at zero and increasing the gains of the BFO and buffer amplifier slightly. If the BFO is zeroed properly no motion will appear in the oscilloscope voltage waveforms. If motion is present, adjust the zero set knob located below the BFO motor drive until no motion is evident in the oscilloscope voltage waveforms.

11) Observe channel 2 of the oscilloscope (V'_{oe}). If a two channel oscilloscope is being used, remove the 1x probe connected to channel 1 and replace it with a current probe that is monitoring the power stage inductor

current. If other channels are available, leave the 1x prove (V_{oe}) connected to channel 1 of the oscilloscope and monitor the power stage inductor current with another channel.

12) Keeping the magnitude of the injected load voltage (V_{oe}) constant (magnitude of injected voltage indicated by the voltmeter of the wave analyzer), vary the frequency of the BFO over the range of desired measurement. If the inductor current demonstrates that the converter is moving in and out of both modes of operation (continuous and discontinuous conduction) decrease the magnitude of the BFO. Find a BFO amplitude such that for any frequency, the converter is always operating in the desired mode.

Injected load voltage magnitude may vary with frequency so care must be taken to ensure a constant magnitude for all frequencies.

13) It is suggested that the injected voltage to be used for the measurement be no more than 80% of the maximum magnitude determined in the previous step.

It should be noted that a smaller injected sinusoid will provide results that are more valid than a larger injected voltage. The injected voltage should be small to preserve a linear system approximation about the operating point, however, it should be large enough to avoid problems with switching noise. A typical acceptable injected load voltage for output impedance tests would be 1.0-3.0 Volts RMS.

14) If a two channel oscilloscope is being used replace the voltage probe (V_{oe}) to channel 1, reset the gain of channel 1 to that of channel 2, and ac couple channel 1.

15) Place the BFO at the minimum of the desired frequency range. Record the

magnitude of the small signal injected load voltage (V'_{oe}) from channel 2 of the oscilloscope (determined in steps 12, 13). Record the magnitude of the small signal output voltage (V_{oe}) from channel 1 of the oscilloscope.

16) Adjust the frequency of the BFO to the next point of measurement. Adjust the magnitude of the small signal injected load voltage (channel 2) until it is the same as that determined in step 12, 13. Record the magnitude of the small signal output voltage (channel 1).

17) Repeat step 16 until the measurement range is covered. 10-15 data points/decade are suggested with at least half in the first two major divisions.

Evaluation

$$\text{Output Impedance} = 20 \log \left(\frac{R_L V_{oe}}{V'_{oe} + V_{oe}} \right) \text{ dB}$$

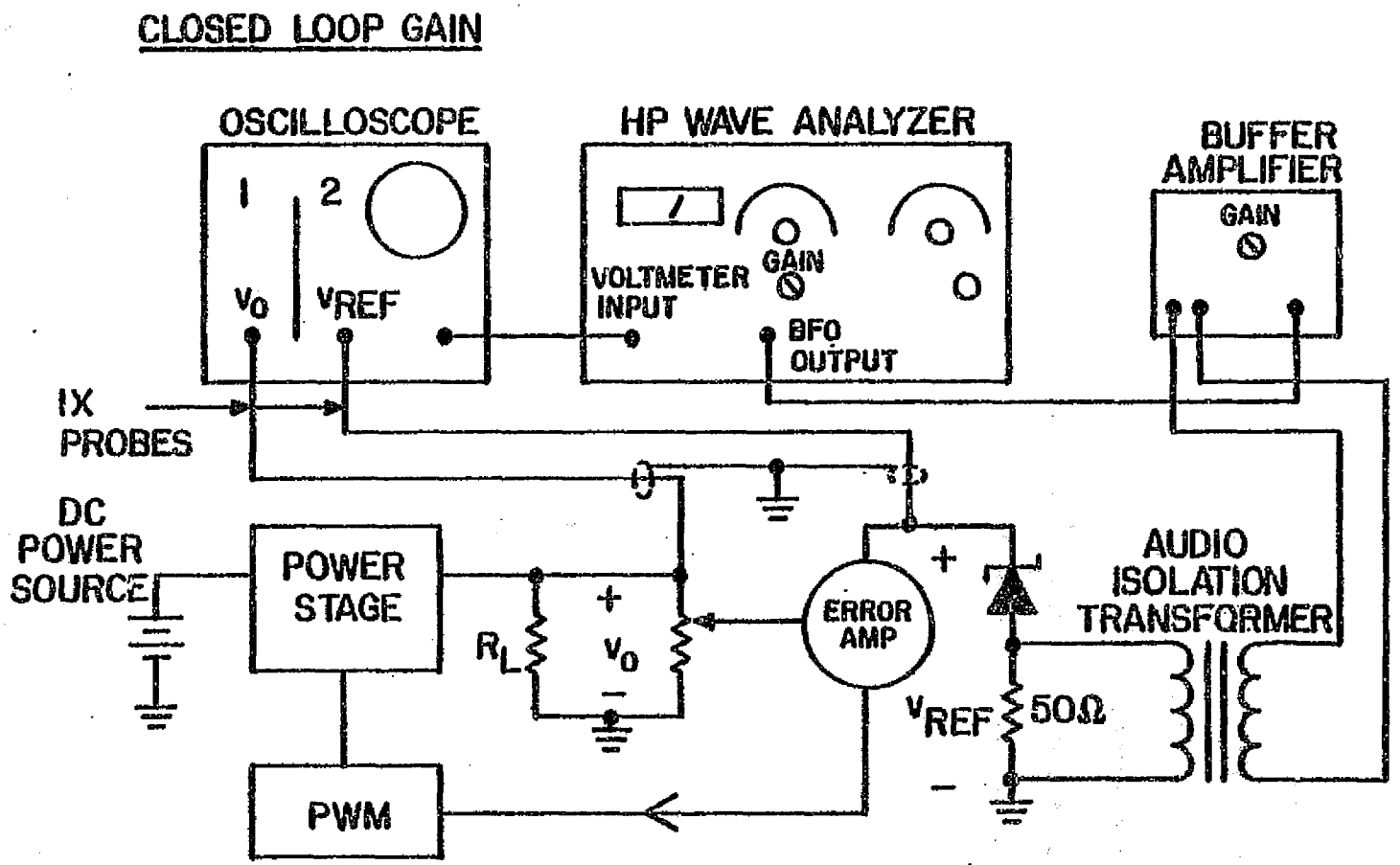

Figure 3.4 Layout diagram for the measurement of closed-loop gain

Normalized Closed-Loop Gain Reference figure 3.4

Equipment

DC power source

2 (or more) channel oscilloscope

Wave analyzer (HP302A or similar)

2 1x voltage probes

Audio isolation transformer (Solar Electronics 6220-1A or similar)

Buffer amplifier (McIntosh 75 or similar)

1 Current probe

Load resistor

1 50 OHM resistor

Procedure

1) Turn all power off.
2) Insert the 50Ω resistor in series between the Zener reference and ground (the figure shows a positive reference but the placement of the 50Ω resistor would be the same if the Zener were inverted and negative reference were used).
3) Place the secondary of the audio isolation transformer across the inserted 50Ω resistor.
4) Connect the output of the beat frequency oscillator (BFO) in the wave analyzer to the input of the buffer amplifier. Turn the gain of the BFO and the gain of the buffer amplifier to zero (full CCW). Do not connect the output of the buffer amplifier to the isolation transformer.
5) Connect the signal out (or vertical out) of the oscilloscope to the input of the frequency selective voltmeter in the wave analyzer. Turn the sensitivity of the voltmeter to the least sensitive position.

6) Place a 1x voltage probe on the reference voltage of the dc-to-dc converter (V_{refe}) and connect this probe to channel 2 of the oscilloscope. Place a different 1x voltage probe on the output voltage of the dc-to-dc converter (V_{oe}) and connect this probe to channel 1 of the oscilloscope. ac couple both inputs. Set the gain of both channels to 0.1-0.2 V/div (equal gains for easier computation). For closed loop gain tests, the oscilloscope is used only as a switch to choose between channel 1 (V_{oe}) or channel 2 (V_{refe}).

7) Turn the converter on.

8) Using a dc voltmeter measure and record the magnitudes of the dc output voltage $V_{O,AVE}$ and the dc reference voltage $V_{REF,AVE}$.

9) Turn on the oscilloscope, wave analyzer, and buffer amplifier.

10) Connect the output of the buffer amplifier to the primary of the audio isolation transformer. This is done after the converter is started to avoid destructive transients passing backward through the isolation transformer and into the output of the buffer amplifier. Warning - If the converter must be shut down, disconnect the primary of the audio isolation transformer before restarting.

11) Check the setup by placing the BFO frequency to 30 of 40 Hz. Increase the gain of the buffer amplifier and the BFO until motion is present in the observed waveforms on the oscilloscope. The magnitude of both waveforms (indicated by the wave analyzer voltmeter) should vary directly with the amplitude of the BFO. If one or both of these tests fails repeat all steps.

12) Zero the BFO by placing the frequency at zero and increasing the gains of the BFO and buffer amplifier slightly. If the BFO is zeroed properly

no motion will appear in the oscilloscope voltage waveforms. If motion is present, adjust the zero set knob located below the BFO motor drive until no motion is evident in the oscilloscope voltage waveforms.

13) Observe channel 2 of the oscilloscope (V_{refe}). If a two channel oscilloscope is being used, remove the 1x probe connected to channel 1 and replace it with a current probe that is monitoring the power stage inductor current. If other channels are available, leave the 1x probe (V_{oe}) connected to channel 1 of the oscilloscope and monitor the power stage inductor current with another channel.

14) Keeping the magnitude of the injected voltage (V_{refe}) constant (magnitude of the injected voltage is indicated by the voltmeter of the wave analyzer) vary the frequency of the BFO over the range of desired measurement. If the inductor current demonstrates that the converter is moving in and out of the both modes of operation (continuous and discontinuous conduction) decrease the magnitude of the BFO. Find a BFO amplitude such that for any frequency, the converter is always operating in the desired mode.

Injected voltage magnitude may vary with frequency so care must be taken to ensure a constant magnitude for all frequency.

15) It is suggested that the injected voltage to be used for the measurement be no more than 80% of the maximum magnitude determined in the previous step.

It should be noted that a smaller injected sinusoid will provide results that are more valid than a larger injected voltage. The injected voltage should be small to preserve a linear system approximation about

the operating point. However, it should be large enough to avoid problem with switching noise. A typical acceptable injected voltage for closed loop gain tests would be 50-200 mV RMS.

16) If a two channel oscilloscope is being used replace the voltage probe (V_{oe}) to channel 1, reset the gain of channel 1 to that of channel 2, and ac couple channel 1.

17) Place the BFO at the minimum of the desired frequency range. Adjust and record the magnitude of the small signal injected voltage (V_{refe}) from channel 2 of the oscilloscope (determined in 13, 14). Record the magnitude of the small signal output voltage V_{oe} from channel 1.

18) Adjust the frequency of the BFO to the next frequency of desired measurement. Adjust the magnitude of the small signal injected voltage (channel 2) until it is the same as that determined in steps 13, 14. Record the magnitude of the small signal output voltage V_{oe} present at channel 1.

19) Repeat step 17 until the measurement range is covered.

10-15 data points/decade are suggested with at least half in the first two major divisions.

Evaluation

$$\text{Normalized Closed-loop gain} = 20 \log \left(\frac{V_{oe}/V_{O,AVE}}{V_{refe}/V_{REF,AVE}} \right) \text{dB}$$

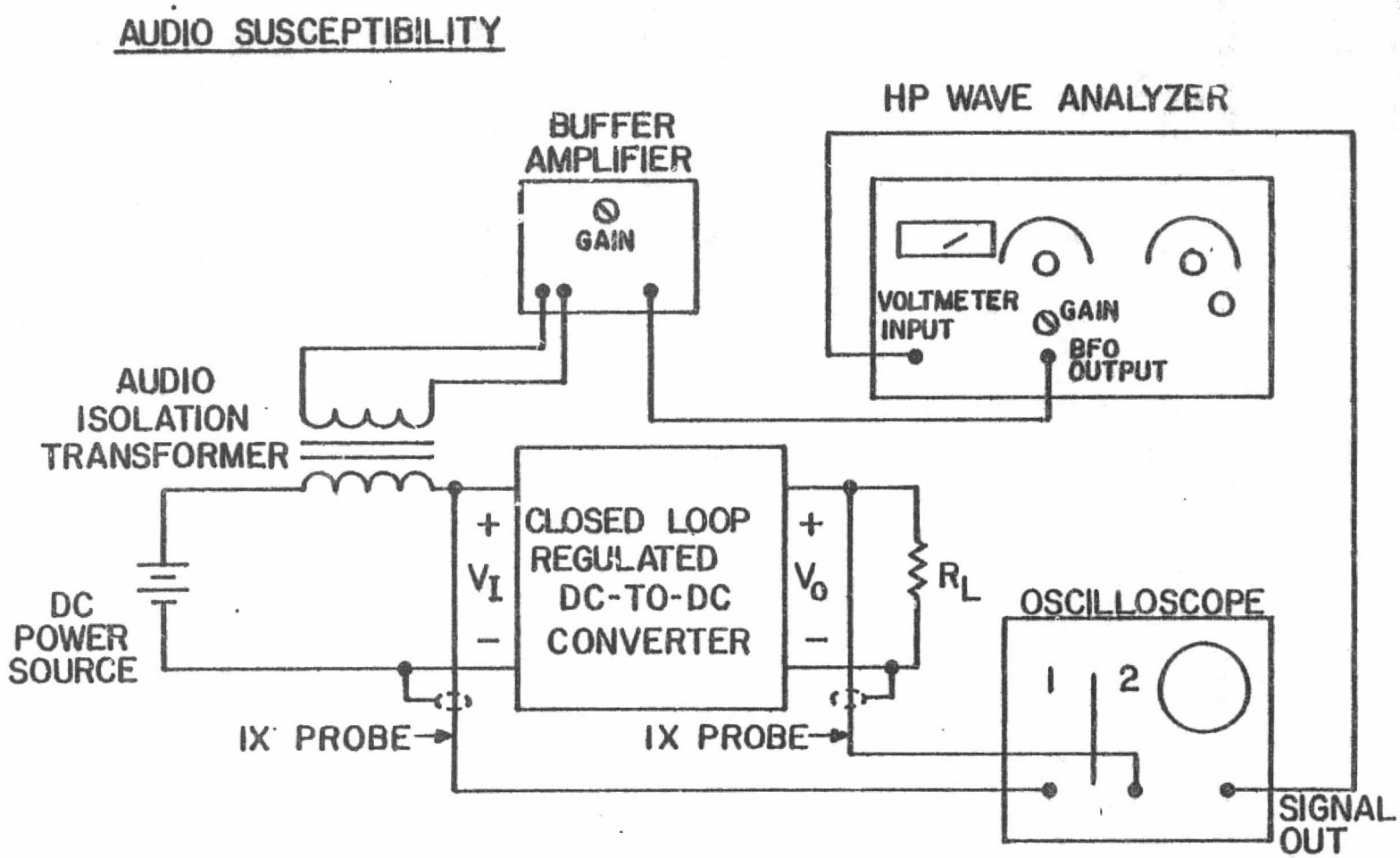

Figure 3.5 Layout diagram for the measurement of audio susceptibility

Audio Susceptibility Reference figure 3.5

Equipment List

DC power source

2 (or more) channel oscilloscope

Wave analyzer (HP 302A or similar)

2 1x voltage probes

Audio isolation transformer (Solar Electronics 6220-1A or similar)

Buffer amplifier (McIntosh 75 or similar)

1 Current probe

Load resistor

Procedure

1) Turn all power off.
2) Place the secondary of the audio isolation transformer in series with the dc power supply and the input to the dc-to-dc converter.
3) Connect the output of the beat frequency oscillator (BFO) from the wave analyzer to the input of the buffer amplifier. Turn the gain of the BFO and the gain of the buffer amplifier to zero (full CCW). Do not connect the output of the buffer amp to the isolation transformer.
4) Connect the signal out (or vertical out) of the oscilloscope to the input of the frequency selective voltmeter in the wave analyzer. Turn the sensitivity of the voltmeter to the least sensitive position.
5) Place a 1x probe on the input voltage (V_{ie}) of the dc-to-dc converter. Connect this probe to channel 1 of the scope. Place a different 1x probe on the output voltage (V_{oe}) of the dc-to-dc converter. Connect this probe to channel 2 of the scope. Set both of the sensitivities of

the two vertical amplifiers to 0.1 or 0.2 V/div (gains should be equal for easier computation). AC couple both inputs.

For audio susceptibility tests, the oscilloscope is used only as a switch to choose between channel 1 (V_{ie}) or channel 2 (V_{oe}).

6) Turn the converter on. Measure and record the dc input voltage ($V_{I,AVE}$) and dc output voltage ($V_{O,AVE}$) of the converter with a dc voltmeter.

7) Connect the output of the buffer amplifier to the primary of the audio isolation transformer. This is done after the converter is started to avoid destructive transients passing backward through the transformer and into the output of the buffer amplifier. Warning - If the converter must be shut down, disconnect the buffer amplifier from the audio isolation transformer before restarting.

9) Check the setup by placing the BFO frequency to 30 or 40 Hz. Increase the gain of the buffer amplifier and the BFO until motion is present in the voltage waveforms on channel 1 and channel 2 of the oscilloscope. The magnitude of both waveforms (indicated by the wave analyzer voltmeter) should vary directly with the amplitude of the BFO. If one or both of these tests fail repeat all steps.

10) Zero the BFO by placing the frequency at zero and increasing the gains of the BFO and buffer amplifier slightly. If the BFO is zeroed properly no motion will appear in the oscilloscope voltage waveforms. If motion is present, adjust the zero set knob below the BFO motor drive until no motion is evident in the oscilloscope voltage waveforms.

11) Observe channel 1 of the oscilloscope (V_{ie}). If a two channel oscilloscope is being used, remove the 1x probe from channel 2 and replace it with a

current probe that is monitoring the power stage inductor current. If other channels are available, leave the 1x probe (V_{oe}) connected to channel 2 and monitor the power stage inductor current with another channel.

12) Keeping the magnitude of the injected voltage (channel 1) constant (magnitude of injected voltage indicated by the voltmeter of the wave analyzer), vary the frequency of the BFO over the range of desired measurement. If the inductor current demonstrates that the converter is moving in and out of both modes of operation (continuous and discontinous conduction) decrease the magnitude of the BFO. Find a BFO amplitude such that for any frequency, the converter is always operating in the desired mode.

Injected voltage may vary with frequency so care must be taken to ensure a constant magnitude for all frequency.

13) It is suggested that the injected voltage to be used for the measurement be no more than 80% of the maximum magnitude determined in the previous step.

It should be noted that a smaller injected sinusoid will provide results that are more valid than a larger injected voltage. The injected voltage should be small to preserve a linear system approximation about the operating point, however, it should be large enough to avoid problems with switching noise. A typical acceptable injected voltage for audio susceptibility would be 0.5-1.0 Volts RMS.

14) If a two channel oscilloscope is being used replace the output voltage probe (V_{oe}) to channel 2, reset the gain of channel 2 to that of channel 1, and ac couple channel 2.

15) Place the BFO at the minimum of the desired frequency measurement range. Record the magnitude of the small signal injected voltage (V_{ie}) from channel 1 of the oscilloscope (determined in steps 12, 13). Record the magnitude of the small signal output voltage (V_{oe}) from channel 2 of the oscilloscope.

16) Adjust the frequency of the BFO to the next point of desired measurement. Adjust the magnitude of the small signal injected voltage (channel 1) until it is the same as that determined in steps 12, 13. Record the magnitude of the small signal output voltage (channel 2).

17) Repeat (16) until the measurement range is covered.

10-15 Data points/decade are suggested with at least half in the first two major divisions.

Evaluation

$$\text{Audio Susceptibility} = 20 \log \left(\frac{V_{oe}/V_{O,AVE}}{V_{ie}/V_{I,AVE}} \right) \text{ dB}$$

CHAPTER IV

EXPERIMENTAL AND ANALYTICAL RESULTS AND COMPARISON

Introduction

To verify the experimental procedures for measuring small-signal frequency-domain transfer functions of converters two regulated energy-storage dc-to-dc converters were constructed and evaluated. The evaluation of each converter consisted of applying the measurement techniques described earlier in this work to provide experimental transfer functions and also by obtaining theoretical transfer functions using a PDP 11/45 computer to perform the necessary calculations given the converter element specifications.

One converter was a voltage step-up converter operating with constant-frequency feedback control (FQVU). The input voltage varied between 16 and 24 volts with an output voltage of 28 volts. The output power was 10 to 100 watts and the frequency of control was 10 kHz. The second converter was a current step-up constant frequency converter (FQCU) operating with an input voltage between 16 and 24 volts, an output voltage of 12 volts, an output power between 10 and 50 watts and a control frequency of 10 kHz. Schematic diagrams of the power stages of each converter are shown in figures 4.1 and 4.2. The controller is identical for each converter except for the setting of the output voltage sense potentiometer (attenuaton ratio β). The schematic diagram of the feedback controller is included in the analytical derivation section figure 2.2. Each converter was measured and analyzed in both the continuous inductor current mode and in the discontinuous

inductor current mode. The circuit element values and externally imposed operating conditions for each converter operating in each different mode are shown below figures 4.1 and 4.2.

The computer aided analysis was accomplished by a program adapted from software written by J. G. Ferrante [4]. The program in its modified form consists of a section that by entering the power stage configuration and circuit element values including losses will provide the power stage small-signal transfer functions; V_0 (s) / A (s), V_0 (s) / V_I (s), V_0 (s) / I_0 (s). These transfer functions are in the frequency domain and are in the form of a numerator polynomial divided by a denominator polynomial. Each of the power stage transfer functions is then assigned to a unique block within the program. Another section of the program allows the configuring of these blocks to construct feedback systems. The program has the capability to add, subtract, multiply or divide any block by any other block. Also available is the option to close a feedback loop with a block in the forward path and a different block in the return path.

The transfer function $A(s)/V_0(s)$ associated with the controller for each of the converter power stages is entered as two separate blocks. The attenuator ratio β is represented by the first block. The second block is H_F and is the lumped gain of the error amplifier and pulse-width-modulator. These two gains are assumed to be independent of frequency for this particular controller. These controller transfer functions are separated to allow access to the reference voltage for closed-loop gain calculations. The product of the two controller transfer functions is the ratio of the duty cycle A to the converter output voltage V_0, $\beta H_F = A(s)/V_0(s)$, and is calculated in chapter II.

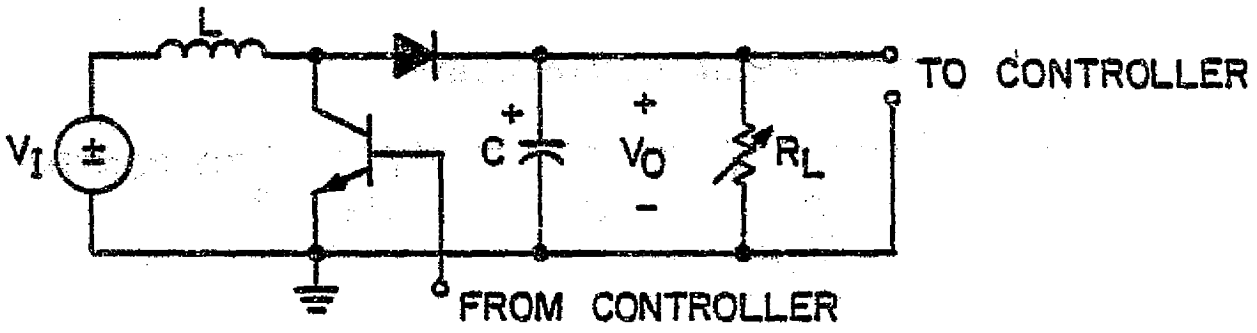

Figure 4.1 Power stage of the constant-frequency voltage step-up converter (FQVU) used with the controller of figure 2.2 for experimental-analytical comparison.

Transistor	2N6354
Diode	1N3879
Capacitor	2000 μF electrolytic
Inductor	0.243 mH (40 turns of #15 AWG on Magnetics core 55019)
V_I	20 V
V_O	28 V
Load Resistor	14 Ω for continuous conduction 40 Ω for discontinuous conduction

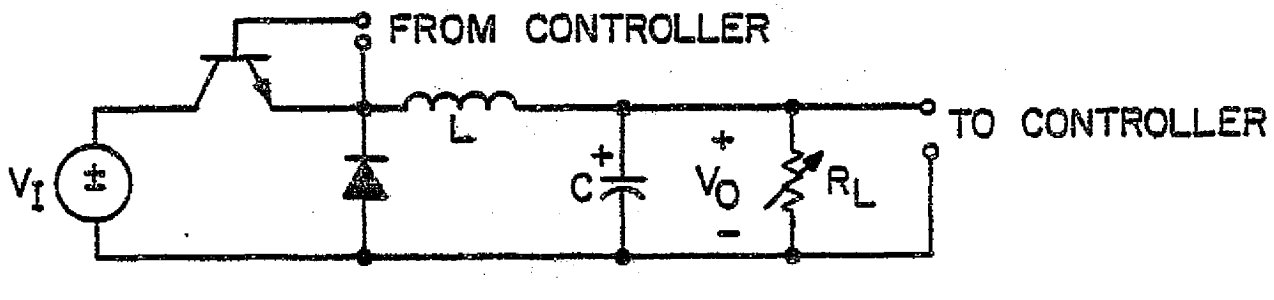

Figure 4.2 Power stage of the constant-frequency current step-up converter (FQCU) used with the controller of figure 2.2 for experimental-analytical comparison.

Transistor	2N3713
Diode	1N3879
Capacitor	1000 μF electrolytic
Inductor	0.279 mH (31 turns of two strands of #16 AWG on Magnetics core 55086)
V_I	24 V
V_O	12 V
Load Resistor	8 Ω for continuous conduction 18 Ω for discontinuous conduction

Figure 4.3 shows the configuring of the frequency dependent blocks within the computer analysis. Figure 4.3a is the block diagram for loop gain and consists of the gain of the feedback controller βH_F multiplied by the power stage gain $V_0(s)/A(s)$. Figure 4.3b is the block diagram for output impedance which relates V_{oe} to I_{oe}. The output impedance requires a closed-loop configuration. Figure 4.3c is also a closed-loop configuration and provides the small-signal normalized closed-loop gain of the dc-to-dc converter, in other words, the susceptibility of the output voltage to disturbances in the reference voltage. Figure 4.3d is the block diagram for audio susceptibility and is also a closed-loop configuration.

Following figure 4.3 are four analytical-experimental comparison sections. They are the constant-frequency voltage step-up converter (FQVU) operating in the continuous conduction mode (mode 1) and in the discontinuous conduction mode (mode 2), and the constant-frequency current step-up converter (FQCU) operating in mode 1 and mode 2. Each section begins with a parameter specification sheet. These parameters were obtained from the physical circuits and entered into the computer to allow the calculation of the various power-stage frequency-domain transfer functions. The parameter sheets are followed by tabular and graphical comparisons between the measured and calculated transfer functions of the four circuits. Included below each tabular comparison are the coefficients of the frequency domain transfer function as calculated by the computer analysis program. These coefficients are to be placed in the following equation.

$$\frac{a_0 + a_1 s + a_2 s^2 \cdots + a_n s^n}{b_0 + b_1 s + b_2 s^2 \cdots + b_m s^m}$$

(a) Loop gain

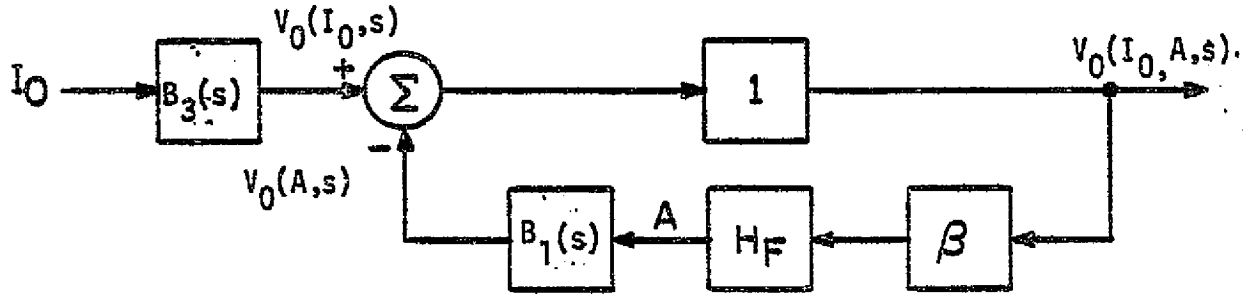

(b) Output impedance

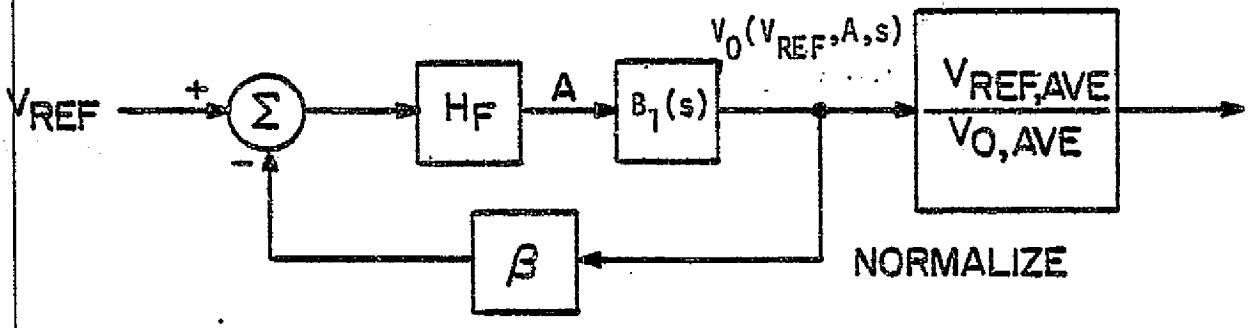

(c) Closed-loop gain

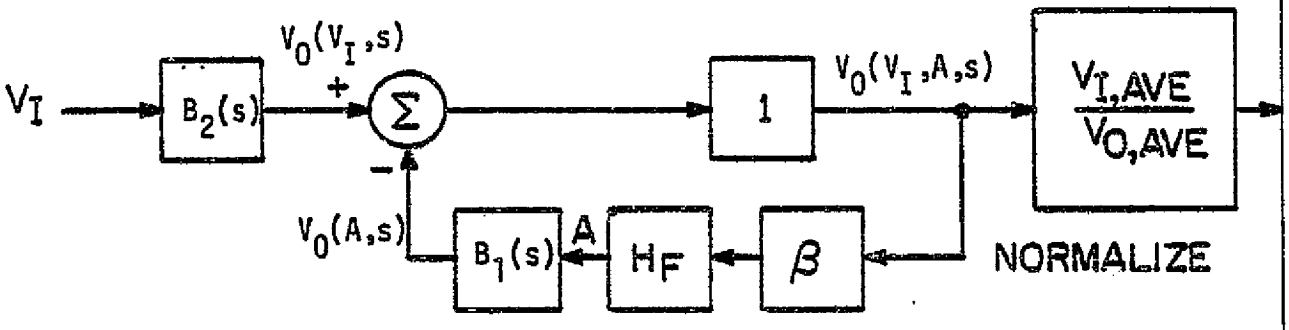

(d) Audio susceptibility

Figure 4.3 The configuring of the frequency dependent blocks within the computer analysis.

$B_1(s) = V_0(s)/A(s)$; $V_I(s), I_0(s)=0$

$B_2(s) = V_0(s)/V_I(s)$; $A(s), I_0(s)=0$

$B_3(s) = V_0(s)/I_0(s)$; $V_I(s), A(s)=0$

For the reasons explained in the first section of chapter II the computer analysis is valid only to half of the switching frequency. For the particular converter-controller combinations under investigation here, half the switching frequency is 5 kHz. For this reason the experimental measurements are only taken up to 5 kHz and the computer generated data can only be interpreted up to 5 kHz.

A brief discussion follows the comparison section.

Constant-Frequency Voltage Step-Up Converter (FQVU) Operating in the Continuous Conduction Mode (Mode 1)

converter frequency	10kHz
L, energy storage inductor	0.243 mH
r_X, winding resistance	0.016 Ω
C, filter capacitor	2000 μF
r_C, equivalent series resistance	0.19 Ω
R_L, load resistance	14 Ω
V_I, input voltage	20 V
v_O, output voltage	28 V
r_Q, saturation resistance	0.1 Ω
r_D, diode ac resistance	0.25 Ω
V_D, diode forward drop	0.7 V

Table 4.1

Loop Gain FQVU Mode 1 (Magnitude, Phase)

Injected Voltage = 100 mV

Frequency (Hz)	Measured (dB,°)	Calculated (dB,°)
20	26.2 ∠ 0°	27.3 ∠ -8°
60	24.8 ∠ -16°	27.1 ∠ -26°
100	22.8 ∠ -44°	26.6 ∠ -42°
140	20.4 ∠ -55°	24.8 ∠ -63°
180	19.0 ∠ -70°	22.3 ∠ -74
250	16.0 ∠ -82°	19.0 ∠ -88°
400	11.9 ∠ -94°	13.6 ∠ -94°
600	7.5 ∠ -104°	8.6 ∠ -90°
800	4.4 ∠ -109°	5.6 ∠ -85°
1000	2.1 ∠ -113°	3.0 ∠ -77°
1400	-1.1 ∠ -120°	0.8 ∠ -70°
1600	-2.2 ∠ -122°	-0.2 ∠ -66°
2500	-5.6 ∠ -133°	-2.8 ∠ -53°
3500	-7.6 ∠ -144°	-4.5 ∠ -41°
5000	-9.2 ∠ -155°	-5.4 ∠ -31°

Calculated Transfer Function

$a_0 = 23.35$ $\quad b_0 = 1.0$

$a_1 = 1.018 \times 10^{-2}$ $\quad b_1 = 1.551 \times 10^{-3}$

$a_2 = 4.951 \times 10^{-7}$ $\quad b_2 = 1.052 \times 10^{-6}$

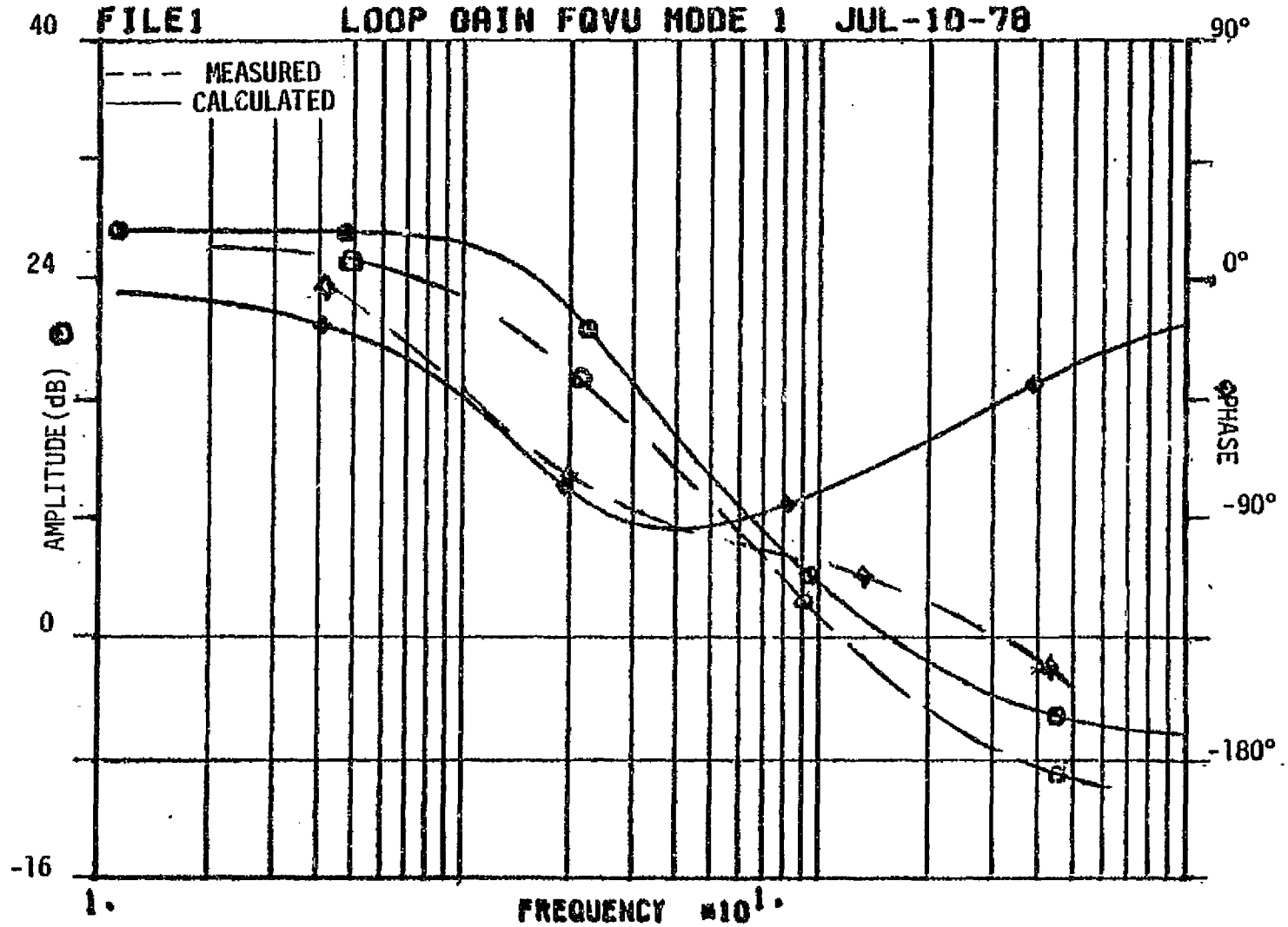

Figure 4.4 Loop gain of a constant-frequency voltage step-up converter operating in the continuous conduction mode. Power stage of figure 4.1, controller of figure 2.2.

Table 4.2

Output Impedance FQVU Mode 1 (Magnitude)

Injected Voltage = 1.0 V

Frequency (Hz)	Measured (dB)	Calculated (dB)
20	-30.0	-33.5
60	-29.5	-32.9
100	-28.4	-32.1
140	-27.5	-30.8
180	-24.6	-25.8
250	-22.5	-27.7
400	-21.1	-24.5
600	-20.7	-22.0
800	-18.8	-20.6
1000	-17.5	-19.6
1400	-15.8	-19.0
2500	-14.5	-18.4
3500	-14.4	-18.3
5000	-14.4	-18.2

Calculated Transfer Function

$a_0 = 5.096 \times 10^{-1}$ $\quad b_0 = 24.35$

$a_1 = 1.492 \times 10^{-3}$ $\quad b_1 = 4.950 \times 10^{-2}$

$a_2 = 1.818 \times 10^{-6}$ $\quad b_2 = 4.536 \times 10^{-5}$

$a_3 = 1.038 \times 10^{-9}$ $\quad b_3 = 1.474 \times 10^{-8}$

$a_4 = 2.033 \times 10^{-13}$ $\quad b_4 = 1.628 \times 10^{-12}$

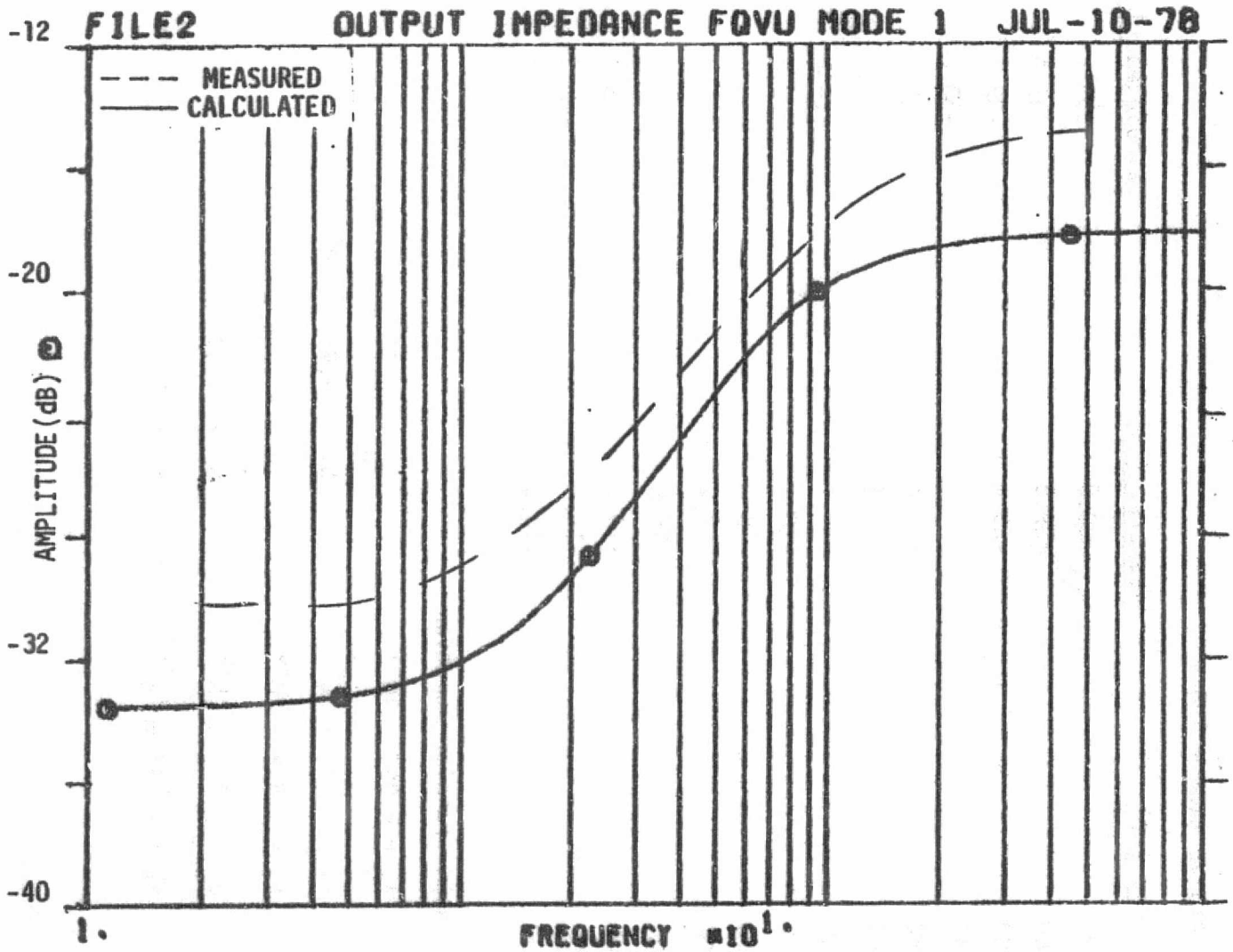

Figure 4.5 Output impedance of a constant frequency voltage step-up converter operating in the continuous conductionmode. Power stage of figure 4.1, controller of figure 2.2. Output impedance in dB referenced to 1 Ω

Table 4.3

Closed-Loop Gain FQVU Mode 1 (Magnitude)

Injected Voltage = 100 mV

Frequency (Hz)	Measured (dB)	Calculated (dB)
20	0.0	0.1
60	0.0	0.13
100	0.0	0.17
140	0.0	0.24
180	0.0	0.29
250	0.1	0.4
400	0.16	0.4
600	0.21	-0.1
800	0.16	-0.9
1000	0.0	-2.1
1400	-0.7	-3.4
2500	-3.1	-6.2
3500	-4.7	-7.4
5000	-6.0	-8.3

Calculated Transfer Function

$a_0 = 690.3$ $\quad b_0 = 681.9$

$a_1 = 3.008 \times 10^{-1}$ $\quad b_1 = 3.284 \times 10^{-1}$

$a_2 = 1.463 \times 10^{-5}$ $\quad b_2 = 4.332 \times 10^{-5}$

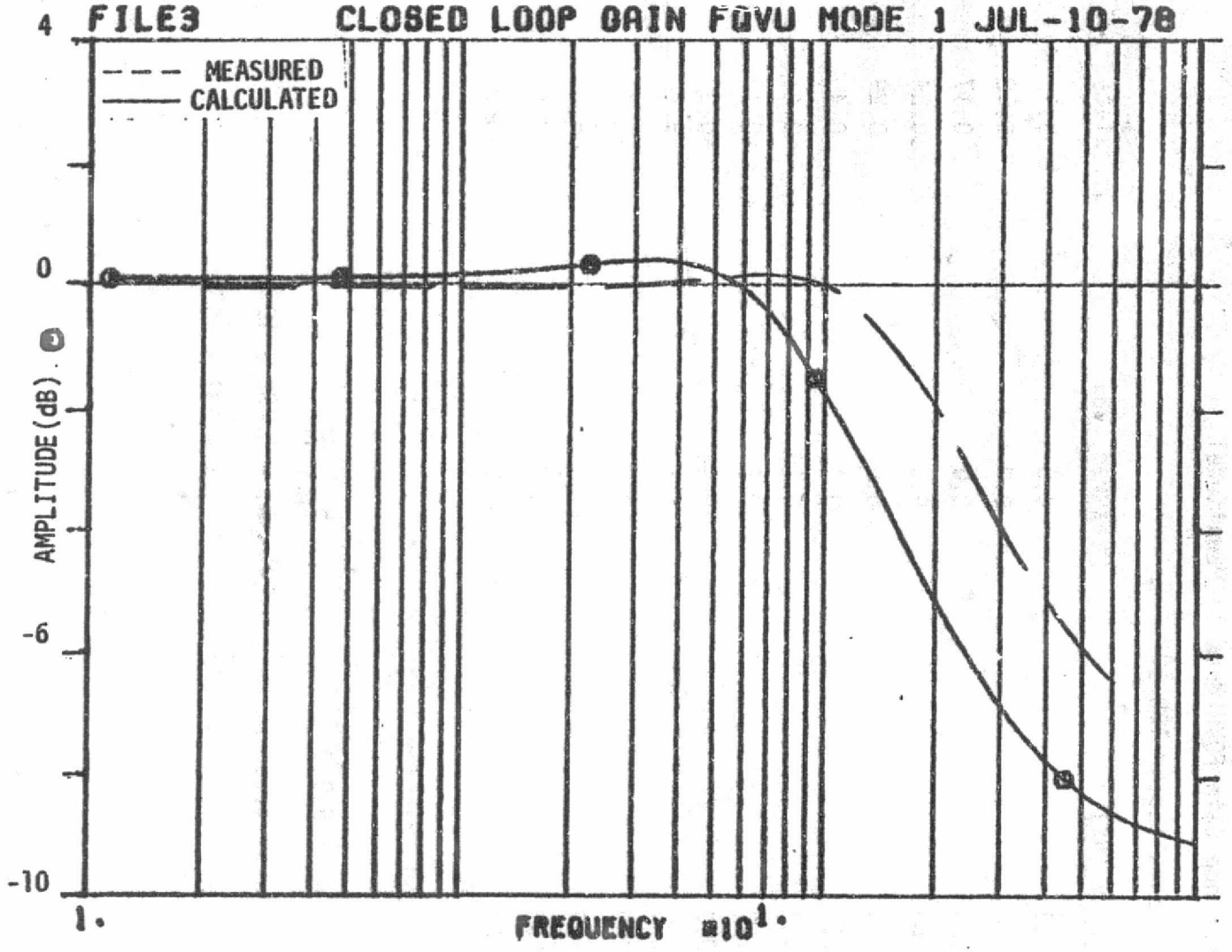

Figure 4.6 Closed-loop gain of a constant-frequency voltage step-up converter operating in the continuous conduction mode. Power stage of figure 4.1, controller of figure 2.2.

Table 4.4

Audio Susceptibility FQVU Mode 1 (Magnitude)

Injected Voltage = 500 mV

Frequency (Hz)	Measured (dB)	Calculated (dB)
20	-25.4	-27.8
60	-25.4	-27.8
100	-25.4	-27.8
140	-25.3	-27.7
180	-25.4	-27.6
250	-25.4	-27.5
400	-25.1	-27.5
600	-25.3	-28.0
800	-25.3	-28.8
1000	-25.5	-30.0
1400	-26.3	-31.3
2500	-29.6	-34.1
3500	-32.6	-35.3
5000	-35.9	-36.3

Calculated Transfer Function

$a_0 = 27.74$ $\quad b_0 = 681.9$

$a_1 = 5.512 \times 10^{-2}$ $\quad b_1 = 1.386$

$a_2 = 4.853 \times 10^{-5}$ $\quad b_2 = 1.270 \times 10^{-3}$

$a_3 = 1.363 \times 10^{-8}$ $\quad b_3 = 4.127 \times 10^{-7}$

$a_4 = 6.188 \times 10^{-13}$ $\quad b_4 = 4.558 \times 10^{-11}$

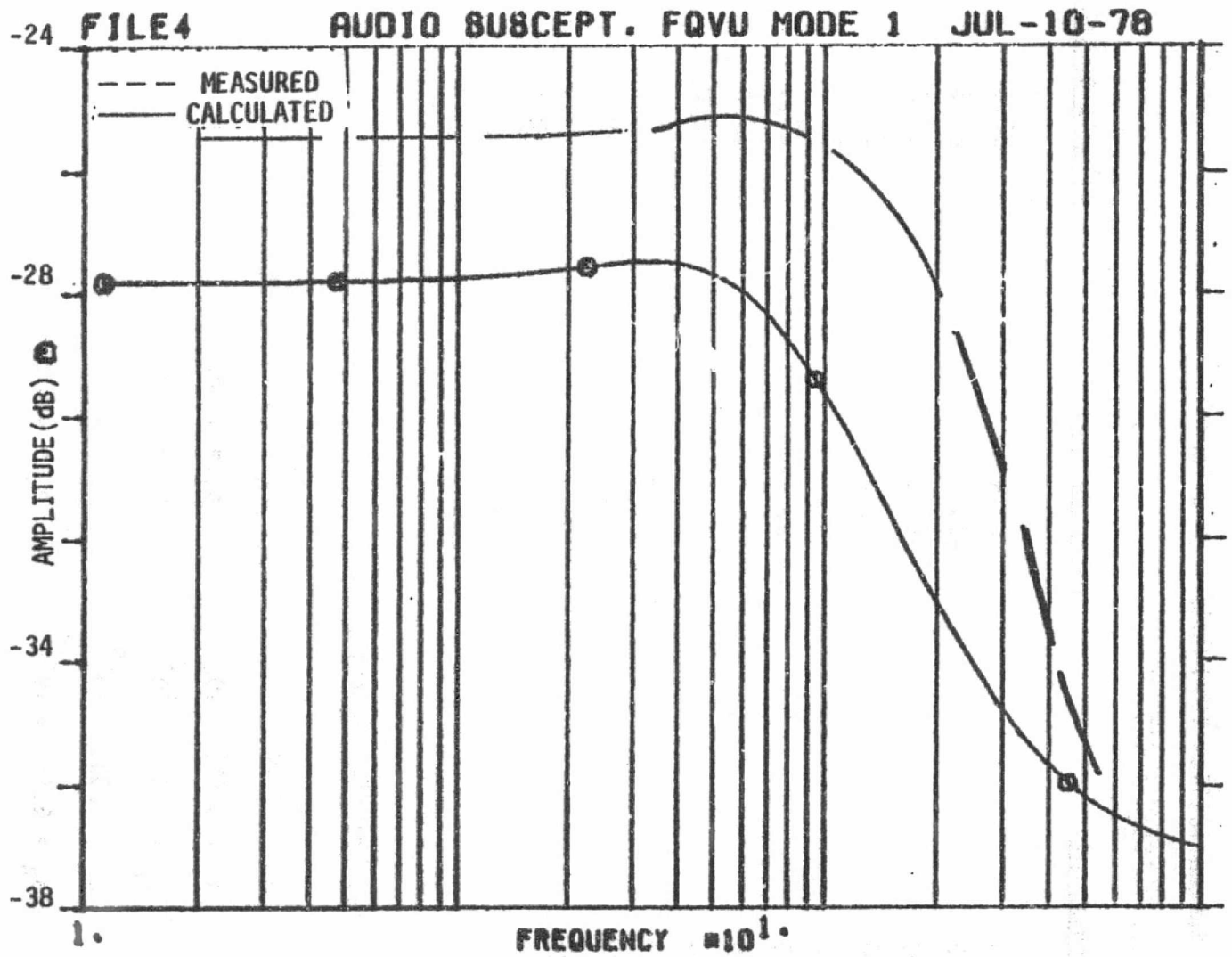

Figure 4.7 Audio susceptibility of a constant-frequency voltage step-up converter operating in the contiuous conduction mode. Power stage of figure 4.1, controller of figure 2.2.

Constant Frequency Voltage Step-Up Converter (FQVU) Operating in the Discontinuous Conduction Mode (Mode 2)

converter frequency	10 kHz
L, energy storage inductor	0.243 mH
r_x, winding resistance	0.016 Ω
C, filter capacitor	2000 μF
r_c, equivalent series resistance	0.19 Ω
R_L, load resistance	40 Ω
V_I, input voltage	20 V
V_O, output voltage	28.2 V
r_O, saturation resistance	0.1 Ω
r_D, diode ac resistance	0.25 Ω
V_D, diode forward drop	0.7 Ω

Table 4.5

Loop Gain FQVU Mode 2 (Magnitude, Phase)

Injected Voltage = 100 mV

Frequency (Hz)	Measured (dB,°)	Calculated (dB,°)
20	25.0 ∠ -43°	21.1 ∠ -64°
60	16.4 ∠ -69°	11.8 ∠ -74°
100	11.9 ∠ -71°	8.3 ∠ -72°
140	9.4 ∠ -69°	5.1 ∠ -68°
180	7.4 ∠ -69°	3.4 ∠ -63°
250	5.0 ∠ -66°	0.9 ∠ -56°
400	2.6 ∠ -60°	-1.4 ∠ -45°
600	0.9 ∠ -53°	-2.9 ∠ -34°
800	0.0 ∠ -57°	-3.6 ∠ -26°
1000	-0.6 ∠ -57°	-4.0 ∠ -21.°
1400	-1.6 ∠ -66°	-4.3 ∠ -16°
1600	-2.2 ∠ -69°	-4.3 ∠ -14°
2500	-3.8 ∠ -86°	-4.5 ∠ -9°
3500	-5.5 ∠ -105°	-4.6 ∠ -6°
5000	-7.9 ∠ -130°	-4.6 ∠ -5°

Calculated Transfer Function

$a_0 = 29.26$ $\quad b_0 = 1.0$

$a_1 = 1.112 \times 10^{-2}$ $\quad b_1 = 1.892 \times 10^{-2}$

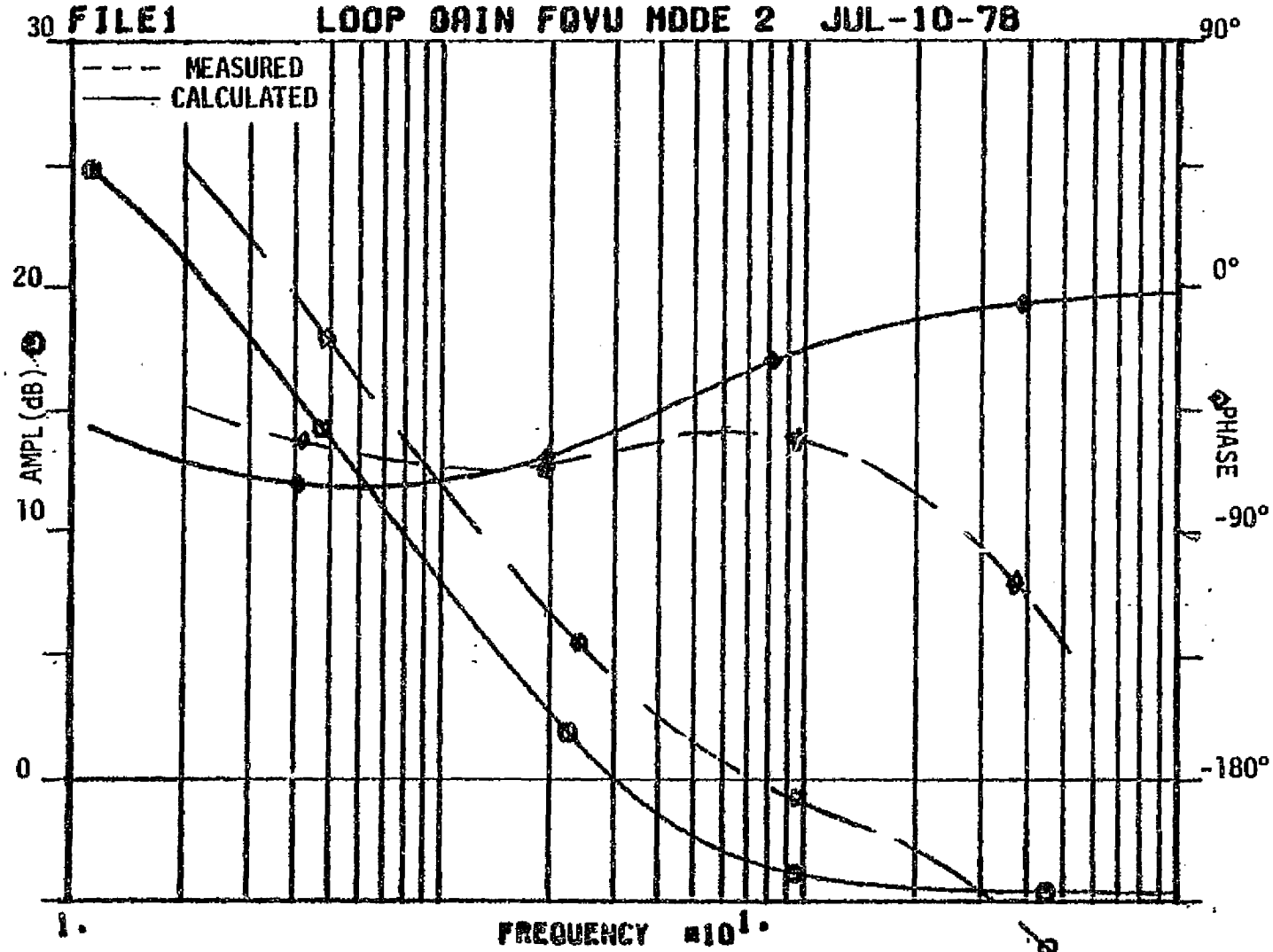

Figure 4.8 Loop gain of a constant-frequency voltage step-up converter operating in the discontinuous conduction mode. Power stage of figure 4.1, controller of figure 2.2.

Table 4.6

Output Impedance FQVU Mode 2 (Magnitude)

Injected Voltage = 1.0 V

Frequency (Hz)	Measured (dB)	Calculated (dB)
20	-12.0	-10.3
60	-12.1	-10.8
100	-12.2	-11.4
140	-13.9	-12.4
180	-14.9	-13.0
250	-15.2	-14.4
400	-16.1	-16.0
600	-17.1	-17.2
800	-18.1	-17.7
1000	-18.4	-18.1
1400	-18.6	-18.3
2500	-19.0	-18.5
3500	-19.1	-18.5
5000	-19.1	-18.6

Calculated Transfer Function

$a_0 = 9.27$ $\quad b_0 = 30.26$

$a_1 = 1.789 \times 10^{-1}$ $\quad b_1 = 6.026 \times 10^{-1}$

$a_2 = 6.665 \times 10^{-5}$ $\quad b_2 = 5.684 \times 10^{-4}$

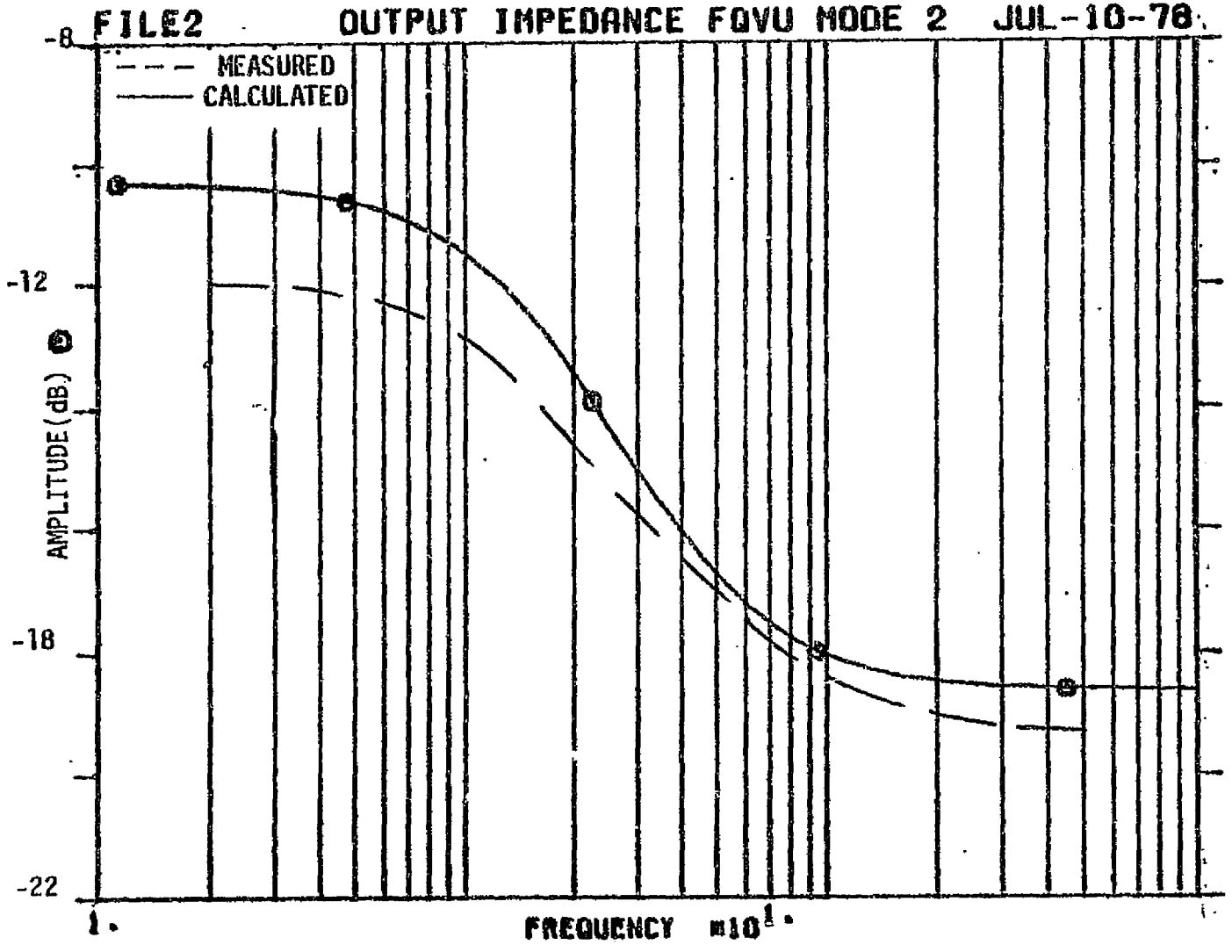

Figure 4.9 Output impedance of a constant-frequency voltage step-up converter operating in the discontinuous conduction mode. Power stage of figure 4.1, controller of figure 2.2. Output impedance in dB referenced to 1 Ω.

Table 4.7

Closed-Loop Gain FQVU Mode 2 (Magnitude)

Injected Voltage = 100 mV

Frequency (Hz)	Measured (dB)	Calculated (dB)
20	0.1	.06
60	-0.1	-0.4
100	-0.3	-1.0
140	-0.7	-2.0
180	-1.1	-2.6
250	-1.9	-4.0
400	-3.1	-5.6
600	-3.9	-6.8
800	-4.3	-7.4
1000	-4.6	-7.7
1400	-4.8	-7.9
2500	-4.9	-8.1
3500	-5.1	-8.1
5000	-5.5	-8.2

Calculated Transfer Function

$a_0 = 864.8$ $\qquad b_0 = 853.2$

$a_1 = 3.286 \times 10^{-1}$ $\qquad b_1 = 8.471 \times 10^{-1}$

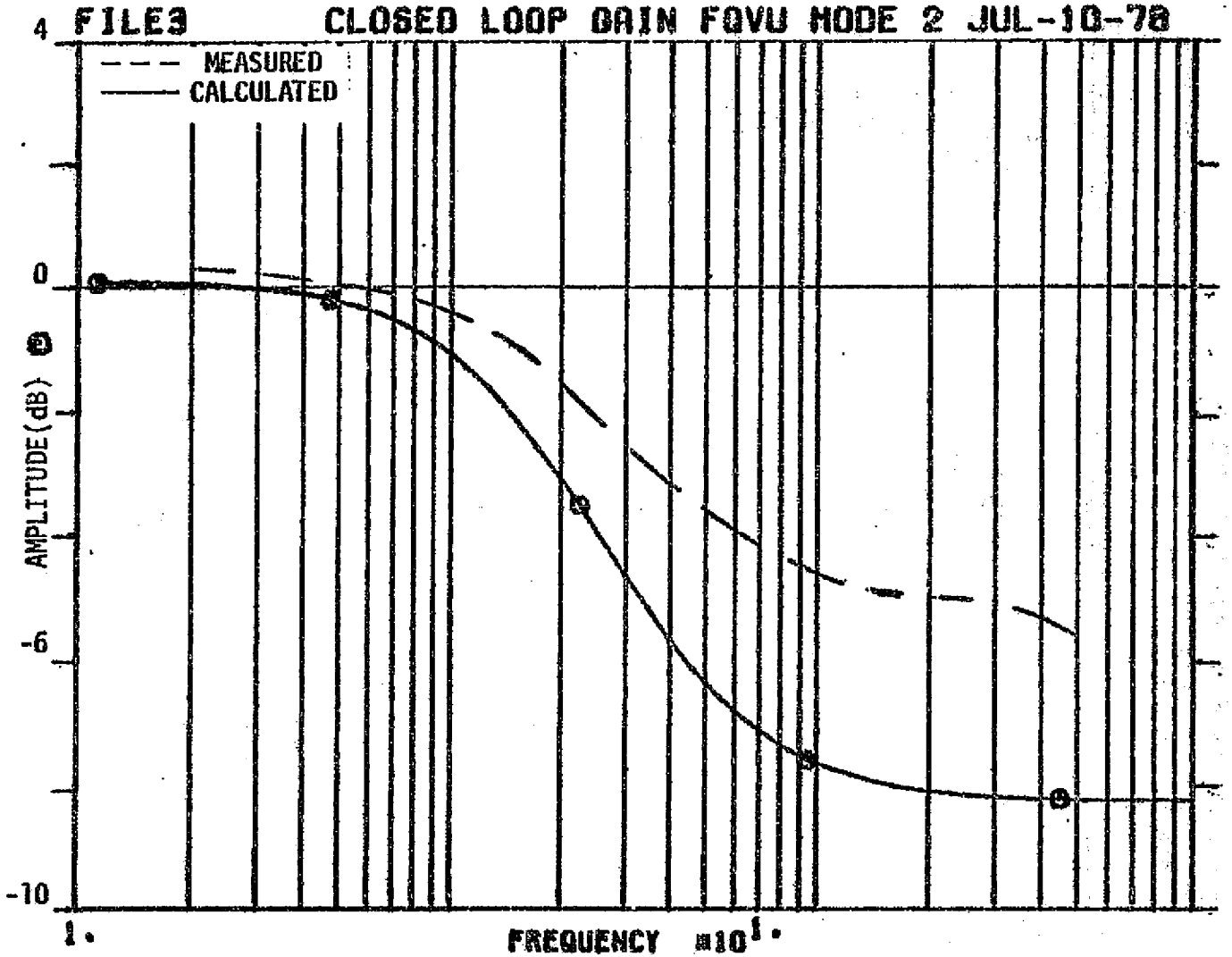

Figure 4.10 Closed-loop gain of a constant-frequency voltage step-up converter operating in the discontinuous mode. Power stage of figure 4.1, controller of figure 2.2.

Table 4.8

Audio Susceptibility FQVU Mode 2 (Magnitude)

Injected Voltage = 500 mV

Frequency (Hz)	Measured (dB)	Calculated (dB)
20	-29.2	-29.5
60	-29.5	-30.0
100	-29.7	-30.5
140	-30.2	-31.5
180	-30.6	-32.3
250	-31.2	-33.6
400	-32.1	-35.2
600	-32.8	-36.4
800	-33.1	-36.9
1000	-33.3	-37.3
1400	-33.5	-37.5
2500	-33.7	-37.6
3500	-34.0	-37.7
5000	-35.1	-37.7

Calculated Transfer Function

$a_0 = 28.84$ $\quad b_0 = 853.2$

$a_1 = 5.567 \times 10^{-1}$ $\quad b_1 = 16.99$

$a_2 = 2.074 \times 10^{-4}$ $\quad b_2 = 1.603 \times 10^{-2}$

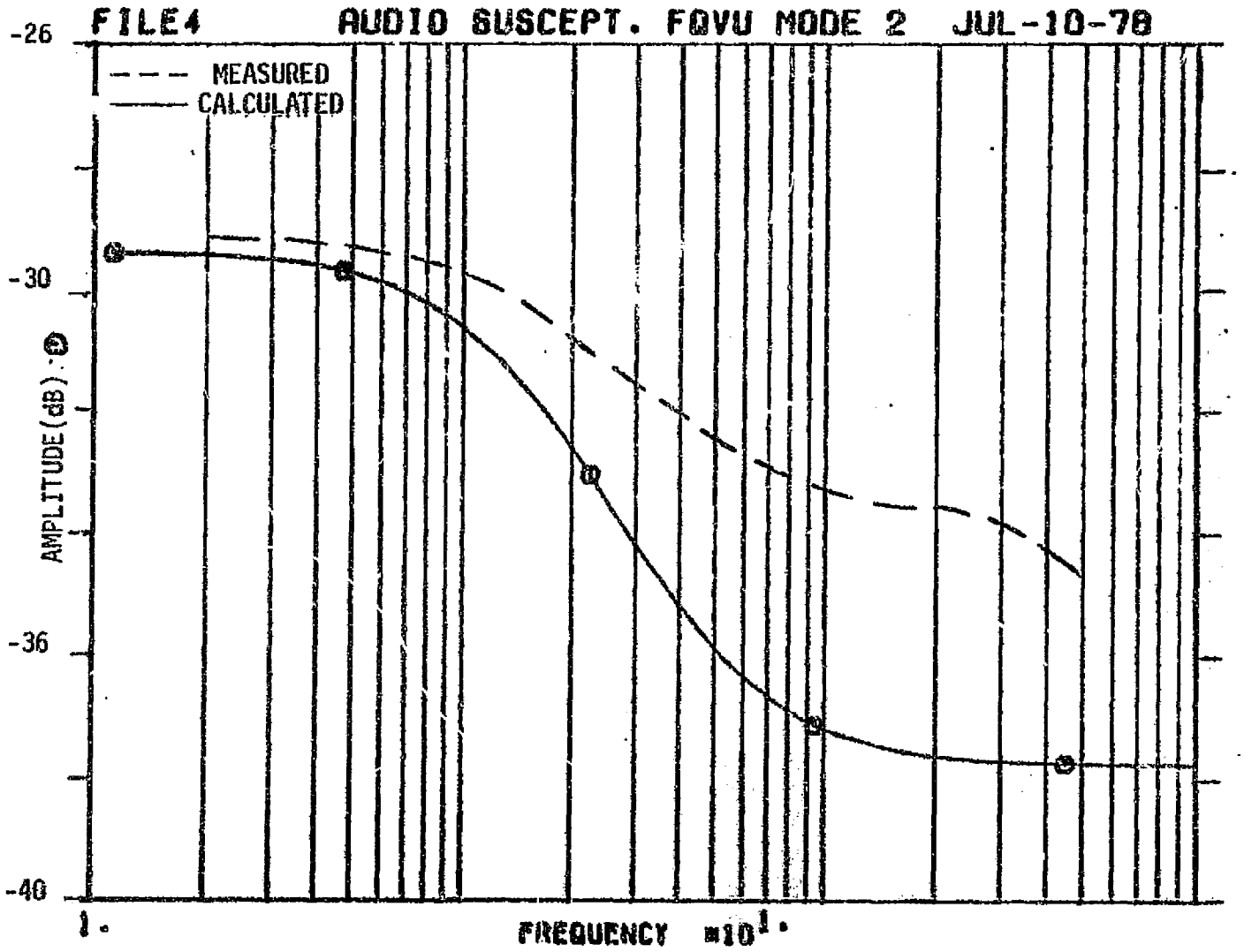

Figure 4.11 Audio susceptibility of a constant-frequency voltage step-up converter operating in the discontinuous conduction mode. Power stage of figure 4.1, controller of figure 2.2.

Constant Frequency Current Step-Up Converter (FQCU) Operating in the Continuous Conduction Mode (Mode 1)

converter frequency	10 KHz
L, energh storage inductor	0.279 mH
r_x, winding resistance	0.02 Ω
C, filter capacitor	1000 μF
r_c, equivalent series resistance	0.1 Ω
R_L, load resistance	8 Ω
V_I, input voltage	24 V
V_O, output voltage	12 V
r_Q, saturation resistance	0.1 Ω
r_D, diode ac resistance	0.25 Ω
V_D, diode forward drop	0.7 V

Table 4.9

Loop Gain FQCU Mode 1 (Magnitude and Phase)

Injected Voltage = 100 mV

Frequency (Hz)	Measured (dB,°)	Calculated (dB,°)
20	29.8 ∠ ---	31.1 ∠ -1°
60	30.1 ∠ ---	31.4 ∠ -5°
100	29.8 ∠ ---	31.8 ∠ -8°
140	29.8 ∠ ---	32.8 ∠ -15°
180	29.3 ∠ -36°	33.7 ∠ -22°
250	27.8 ∠ -66°	35.3 ∠ -54°
400	22.9 ∠ -107°	29.8 ∠ -111°
600	16.6 ∠ -123°	20.8 ∠ -125°
800	11.8 ∠ -130°	15.6 ∠ -123°
1000	8.0 ∠ -130°	11.1 ∠ -116°
1400	3.1 ∠ -131°	7.5 ∠ -106°
2500	-4.7 ∠ -128°	1.5 ∠ -79°
3500	-8.4 ∠ -127°	-0.8 ∠ -60°
5000	-12.5 ∠ -128°	-2.3 ∠ -46°

Calculated Transfer Function

$a_0 = 35.77$ $\quad b_0 = 1.0$

$a_1 = 5.381 \times 10^{-3}$ $\quad b_1 = 3.54 \times 10^{-4}$

$a_2 = 1.804 \times 10^{-7}$ $\quad b_2 = 2.888 \times 10^{-7}$

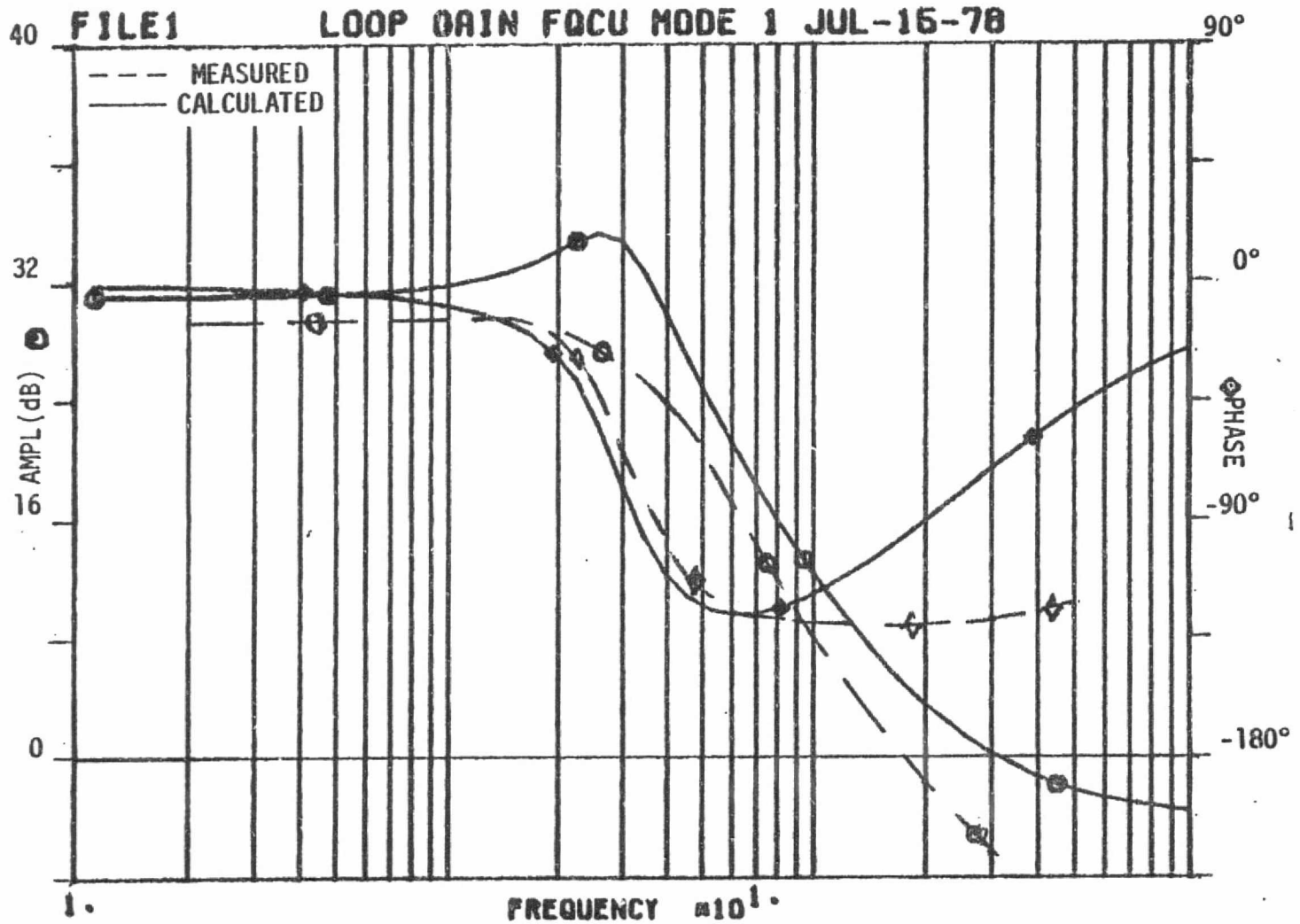

Figure 4.12 Loop gain of a constant-frequency current step-up converter operating in the continuous conduction mode. Power stage of figure 4.2, controller of figure 2.2.

Table 4.10

Output Impedance FQCU Mode 1 (Magnitude)

Injected Voltage = 1.0 V

Frequency (Hz)	Measured (dB)	Calculated (dB)
20	-47.5	-49.5
60	-44.5	-47.1
100	-42.0	-44.9
140	-39.0	-42.3
180	-37.5	-40.5
250	-36.0	-37.8
400	-32.5	-34.0
600	-28.5	-30.1
800	-26.5	-27.5
1000	-23.7	-25.2
1400	-22.0	-23.7
2500	-22.9	-23.4
3500	-23.5	-23.7
5000	-23.2	-24.1

Calculated Transfer Function

$a_0 = 1.182 \times 10^{-1}$ $\quad b_0 = 36.77$

$a_1 = 3.321 \times 10^{-4}$ $\quad b_1 = 1.875 \times 10^{-2}$

$a_2 = 1.648 \times 10^{-7}$ $\quad b_2 = 1.312 \times 10^{-6}$

$a_3 = 9.37 \times 10^{-11}$ $\quad b_3 = 1.823 \times 10^{-9}$

$a_4 = 8.042 \times 10^{-15}$ $\quad b_4 = 1.355 \times 10^{-13}$

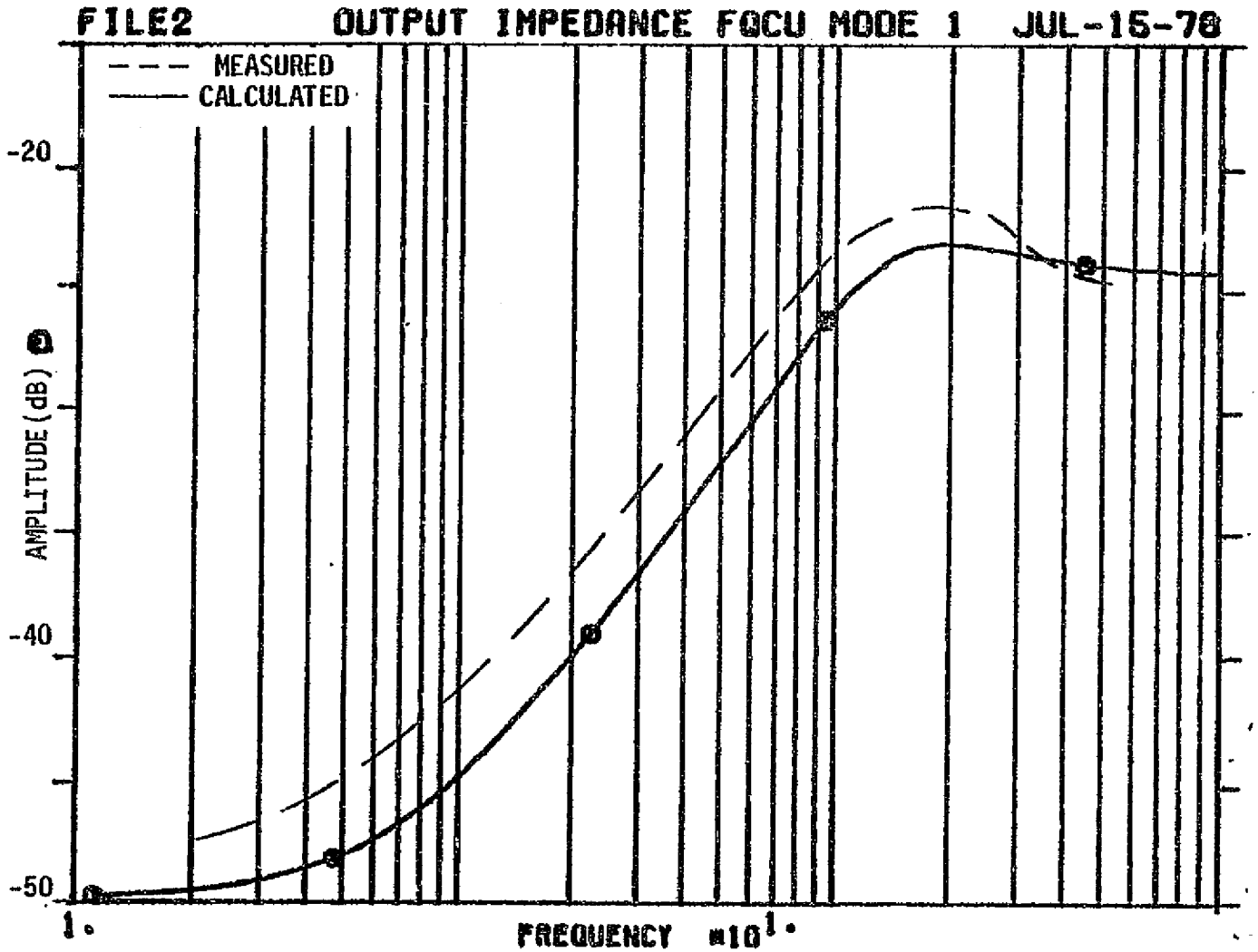

Figure 4.13 Output impedance of a constant-frequency current step-up converter operating in the continuous conduction mode. Power stage of figure 4.2, controller of figure 2.2. Output impedance in dB referenced to 1 Ω.

Table 4.11

Closed-Loop Gain FQCU Mode 1 (Magnitude)

Injected Voltage = 100 mV

Frequency (Hz)	Measured (dB)	Calculated (dB)
20	-0.5	-0.2
60	-0.5	-0.19
100	-0.5	-0.18
140	-0.5	-0.15
180	-0.3	-0.12
250	-0.2	-0.05
400	0.4	0.13
600	1.3	0.5
800	1.0	0.75
1000	-0.4	0.81
1400	-3.8	0.28
2500	-10.0	-3.0
3500	-11.4	-5.0
5000	-12.5	-6.5

Calculated Transfer Function

$a_0 = 431.1$ $\quad b_0 = 441.2$

$a_1 = 6.485 \times 10^{-2}$ $\quad b_1 = 6.882 \times 10^{-2}$

$a_2 = 2.174 \times 10^{-6}$ $\quad b_2 = 5.631 \times 10^{-6}$

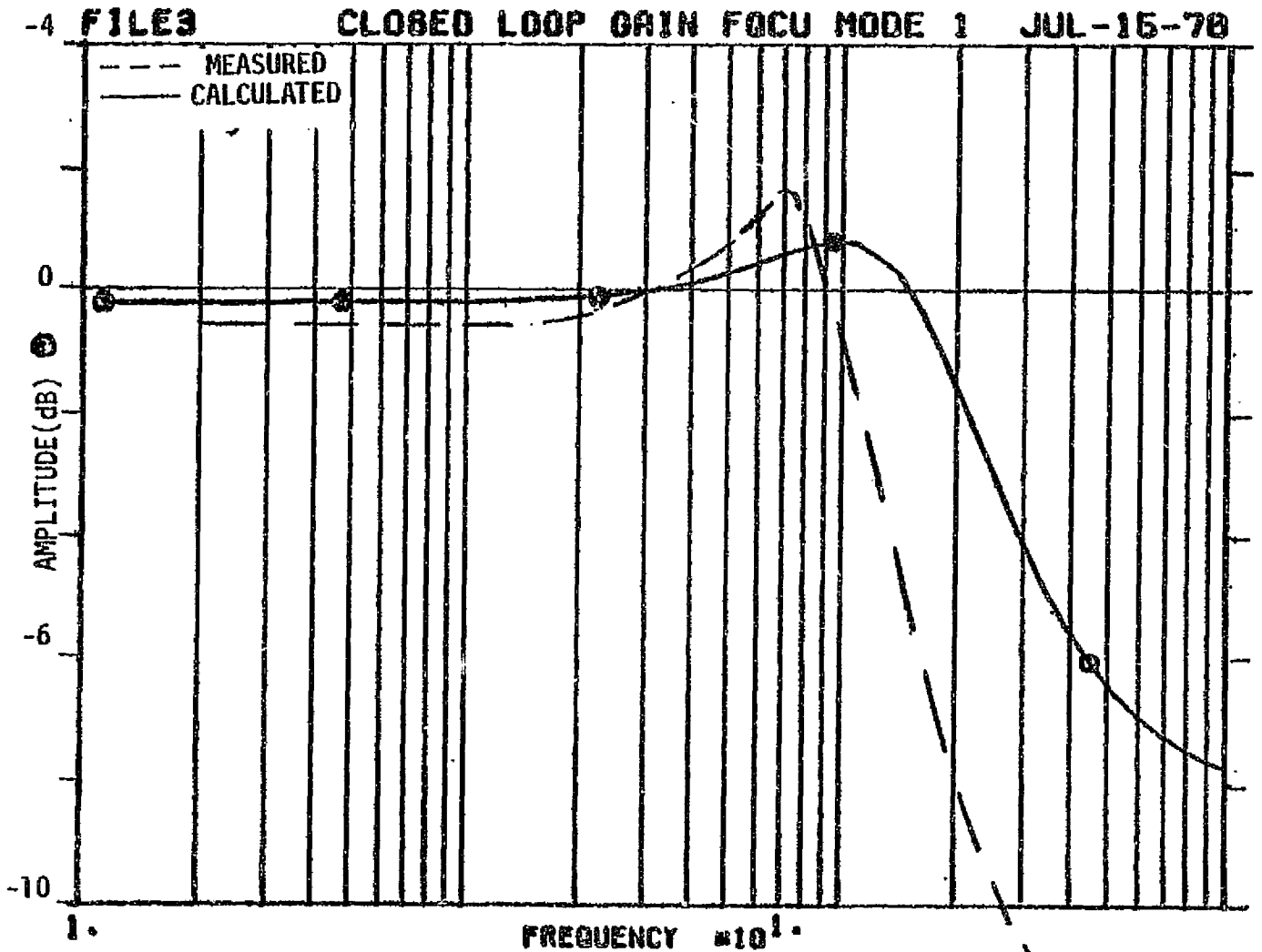

Figure 4.14 Closed-loop gain of a constant frequency current step-up converter operating in the continuous conduction mode. Power stage of figure 4.2, controller of figure 2.2.

Table 4.12

Audio Susceptibility FQCU Mode 1 (Magnitude)

Injected Voltage = 500 mV

Frequency (Hz)	Measured (dB)	Calculated (dB)
20	-31.2	-31.2
60	-31.2	-31.2
100	-31.2	-31.1
140	-31.2	-31.1
180	-31.2	-31.0
250	-31.2	-31.0
400	-31.0	-30.8
600	-30.4	-30.5
800	-30.0	-30.2
100	-29.4	-30.1
1400	-28.5	-30.7
2500	-30.4	-33.9
3500	-34.9	-36.0
5000	-39.3	-37.4

Calculated Transfer Function

$a_0 = 122.1$ $\quad b_0 = 441.2$

$a_1 = 6.161 \times 10^{-3}$ $\quad b_1 = 2.25 \times 10^{-1}$

$a_2 = 4.239 \times 10^{-6}$ $\quad b_2 = 1.574 \times 10^{-4}$

$a_3 = 5.524 \times 10^{-10}$ $\quad b_3 = 2.187 \times 10^{-8}$

$a_4 = 1.779 \times 10^{-14}$ $\quad b_4 = 1.626 \times 10^{-12}$

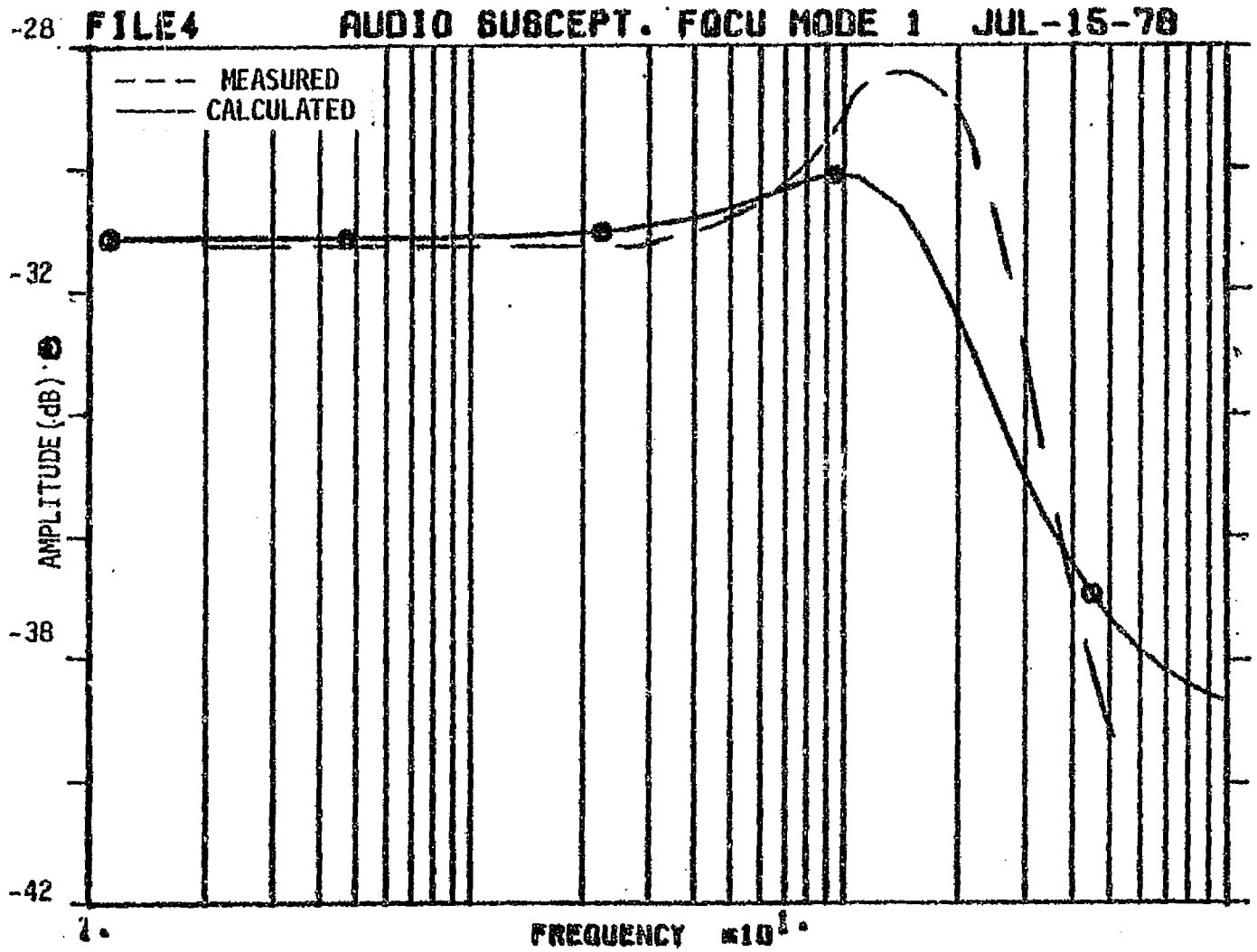

Figure 4.15 Audio susceptibility of a constant-frequency current step-up converter operating in the continuous conduction mode. Power stage of figure 4.2, controller of figure 2.2.

Constant Frequency Current Step-Up Converter (FQCU) Operating in the Discontinuous Conduction Mode (Mode 2)

converter frequency	10 kHz
L, energy storage inductor	.279 mH
r_x, winding resistance	.02 Ω
C, filter capacitor	1000 μF
r_c, equivalent series resistance	0.1 Ω
R_L, load resistance	18 Ω
V_I, input voltage	24 V
V_O, output voltage	12.2 V
r_Q, saturation resistance	0.1 Ω
r_p, diode ac resistance	0.25 Ω
V_D, diode forward drop	0.7 Ω

Table 4.13

Loop Gain FQCU Mode 2 (Magnitude and Phase)

Injected Voltage = 100 mV

Frequency (Hz)	Measured (dB,°)	Calculated (dB,°)
20	27.4 ∠ -133°	27.5 ∠ -36°
60	22.8 ∠ -124°	21.2 ∠ -65
100	19.6 ∠ -109°	17.8 ∠ -71°
140	16.5 ∠ -86°	15.7 ∠ -74°
180	14.1 ∠ -86°	12.7 ∠ -75°
250	10.9 ∠ -87°	9.6 ∠ -75°
400	7.1 ∠ -84°	6.0 ∠ -72°
800	3.0 ∠ -81°	2.7 ∠ -66°
800	0.8 ∠ -79°	0.6 ∠ -61°
1000	-0.9 ∠ -78°	-1.2 ∠ -54°
1400	-3.3 ∠ -77°	-2.6 ∠ -47°
2500	-6.6 ∠ -76°	-4.7 ∠ -32°
3500	-8.6 ∠ -80°	-5.4 ∠ -22°
5000	-10.3 ∠ -88°	-5.8 ∠ -17°

Calculated Transfer Function

$a_0 = 29.68$ $\qquad b_0 = 1.0$

$a_1 = 2.968 \times 10^{-3}$ $\qquad b_1 = 6.06 \times 10^{-3}$

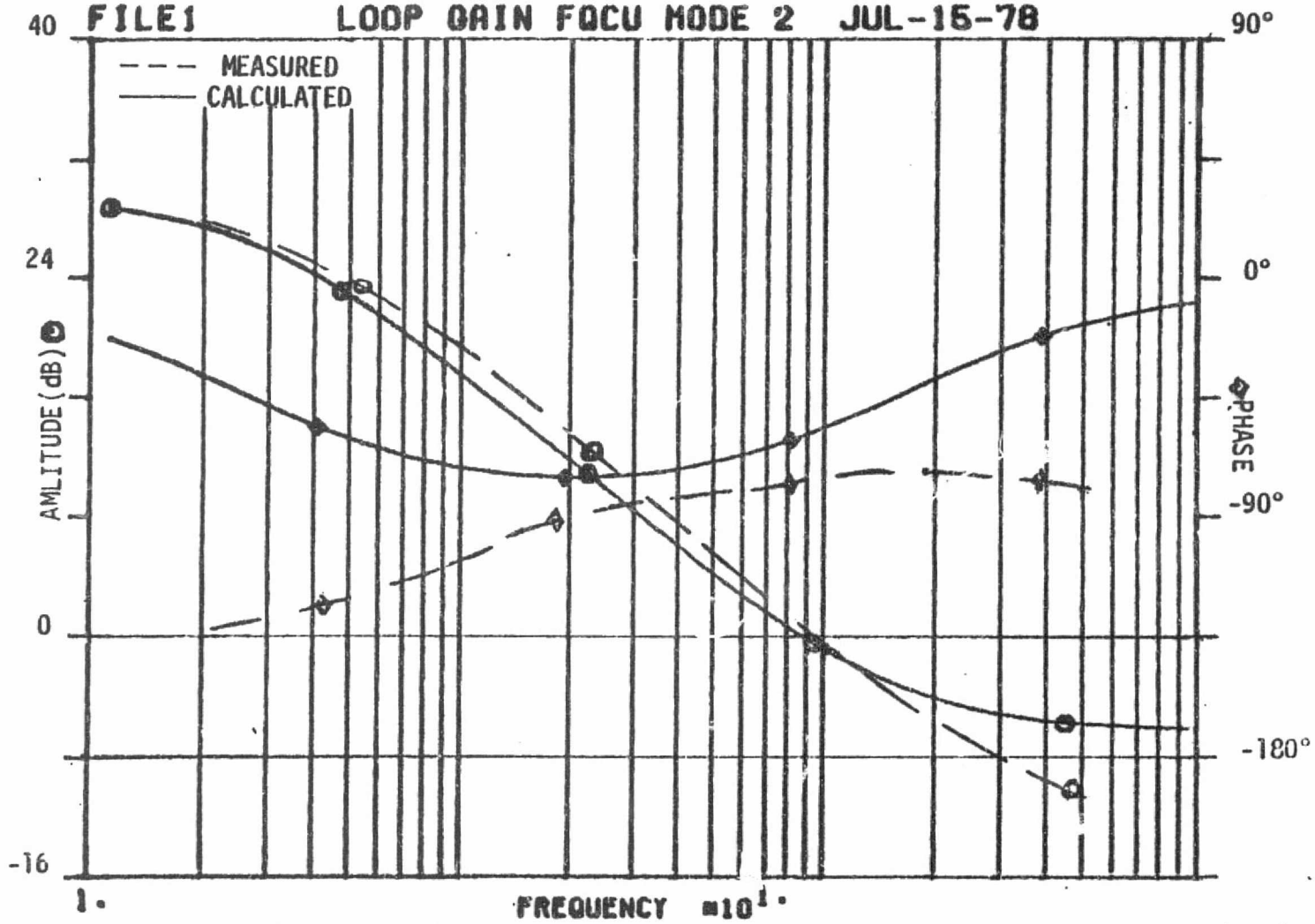

Figure 4.16 Loop gain of a constant-frequency current step-up converter operating in the discontinuous conduction mode. Power stage of figure 4.2, controller of figure 2.2.

Table 4.14

Output Impedance FQCU Mode 2 (Magnitude)

Injected Voltage = 1.0 V

Frequency (Hz)	Measured (dB)	Calculated (dB)
20	-14.5	-14.3
60	-14.5	-14.3
100	-14.5	-14.4
140	-14.5	-14.5
180	-14.2	-14.6
250	-14.6	-15.0
400	-15.6	-15.9
600	-17.0	-17.2
800	-18.2	-18.4
1000	-19.1	-19.6
1400	-20.6	-20.7
2500	-22.3	-22.4
3500	-22.6	-22.9
5000	-23.2	-23.3

Calculated Transfer Function

$a_0 = 5.944$ $\quad b_0 = 30.68$

$a_1 = 3.662 \times 10^{-2}$ $\quad b_1 = 1.95 \times 10^{-1}$

$a_2 = 3.602 \times 10^{-6}$ $\quad b_2 = 5.472 \times 10^{-5}$

ORIGINAL PAGE IS
OF POOR QUALITY

ORIGINAL PAGE IS
OF POOR QUALITY

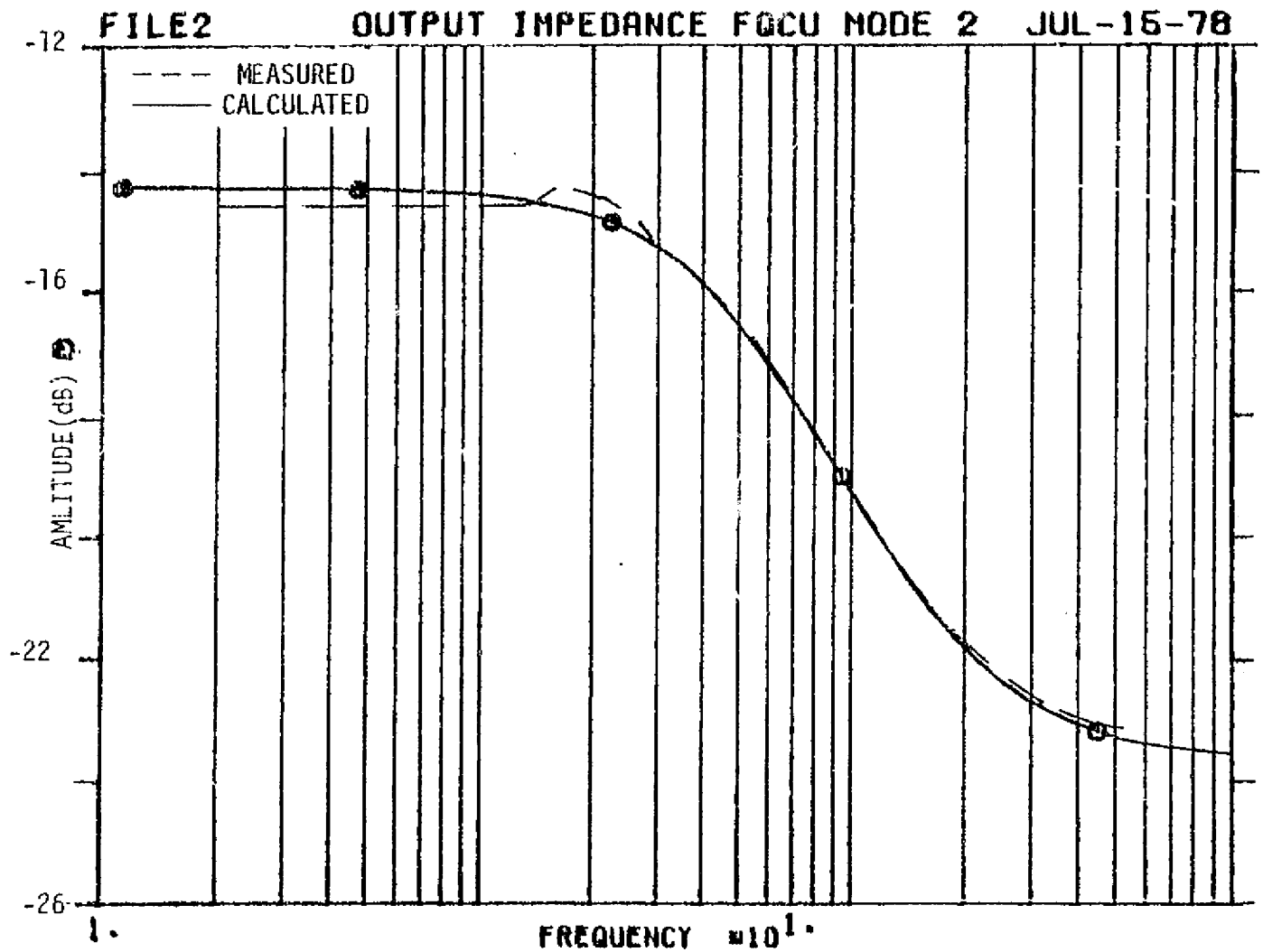

Figure 4.17 Output impedance of a constant-frequency current step-up converter operating in the discontinuous conduction mode. Power stage of figure 4.2, controller of figure 2.2. Output impedance in dB referenced to 1 Ω.

Table 4.15

Closed-Loop Gain FQCU Mode 2 (Magnitude)

Injected Voltage = 100 mV

Frequency (Hz)	Measured (dB)	Calculated (dB)
20	-0.4	-0.4
60	-0.5	-0.43
100	-0.6	-0.52
140	-1.0	-0.7
180	-1.3	-0.8
250	-1.8	-1.2
400	-3.5	-2.0
600	-5.5	-3.4
800	-7.1	-4.5
1000	-8.5	-5.8
1400	-10.2	-6.8
2500	-13.0	-8.5
3500	-14.1	-9.1
5000	-15.6	-9.4

Calculated Transfer Function

$a_0 = 357.7$ $\qquad b_0 = 374.3$

$a_1 = 3.577 \times 10^{-2}$ $\qquad b_1 = 1.101 \times 10^{-1}$

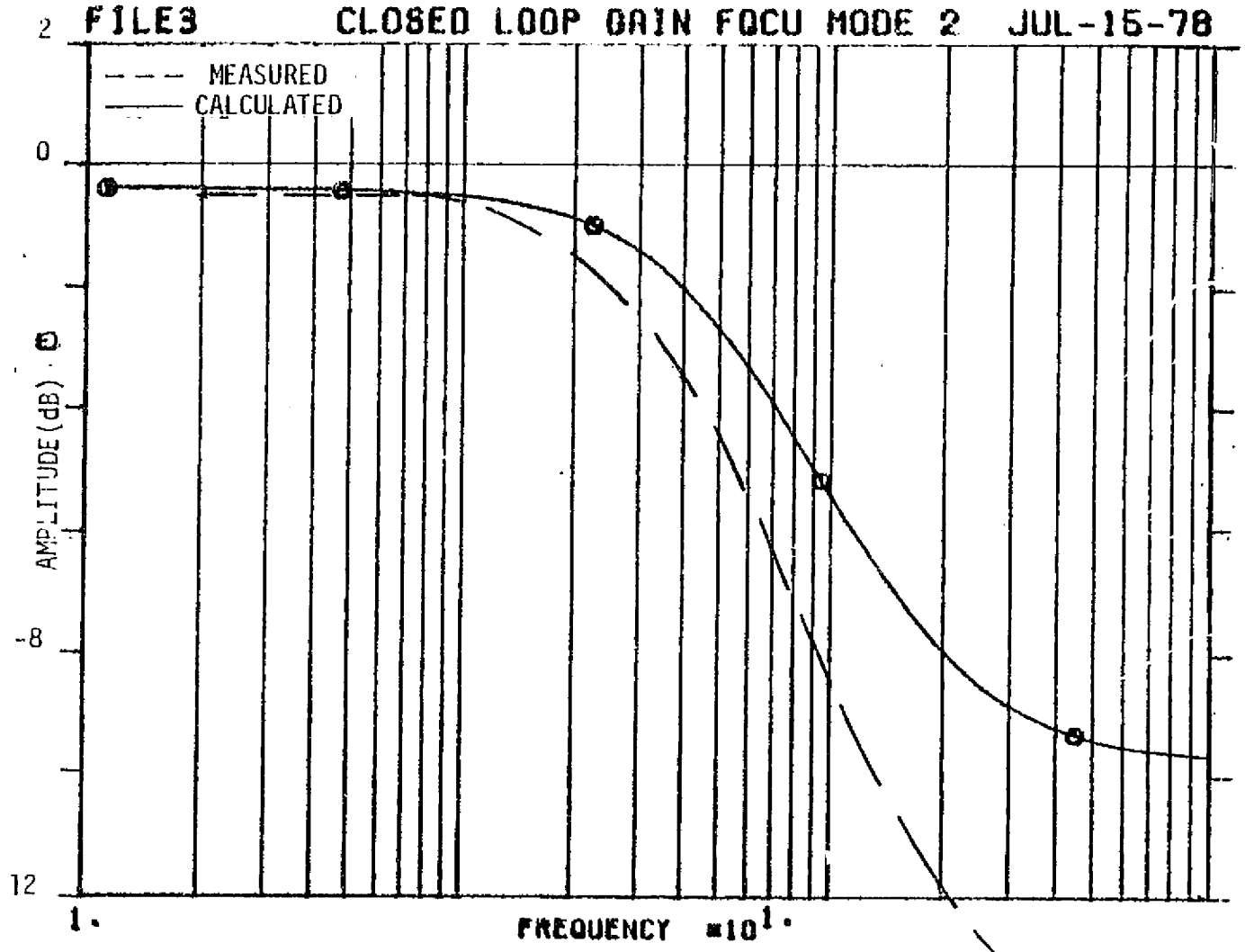

Figure 4.18 Closed-loop gain of a constant-frequency current step-up converter operating in the discontinuous conduction mode. Power stage of figure 4.2, controller of figure 2.2.

Table 4.16

Audio Susceptibility FQCU Mode 2 (Magnitude)

Injected Voltage = 500 mV

Frequency (Hz)	Measured (dB)	Calculated (dB)
20	-30.2	-29.6
60	-30.8	-29.7
100	-31.0	-29.7
140	-31.0	-29.9
180	-31.2	-30.0
250	-31.4	-30.4
400	-31.8	-31.2
600	-33.6	-32.6
800	-34.1	-33.8
1000	-34.1	-35.0
1400	-35.0	-36.0
2500	-37.8	-37.7
3500	-38.8	-38.3
5000	-40.9	-38.6

Calculated Transfer Function

$a_0 = 12.36$ $\quad b_0 = 374.3$

$a_1 = 7.617 \times 10^{-2}$ $\quad b_1 = 2.379$

$a_2 = 7.493 \times 10^{-6}$ $\quad b_2 = 6.675 \times 10^{-4}$

ORIGINAL PAGE IS
OF POOR QUALITY

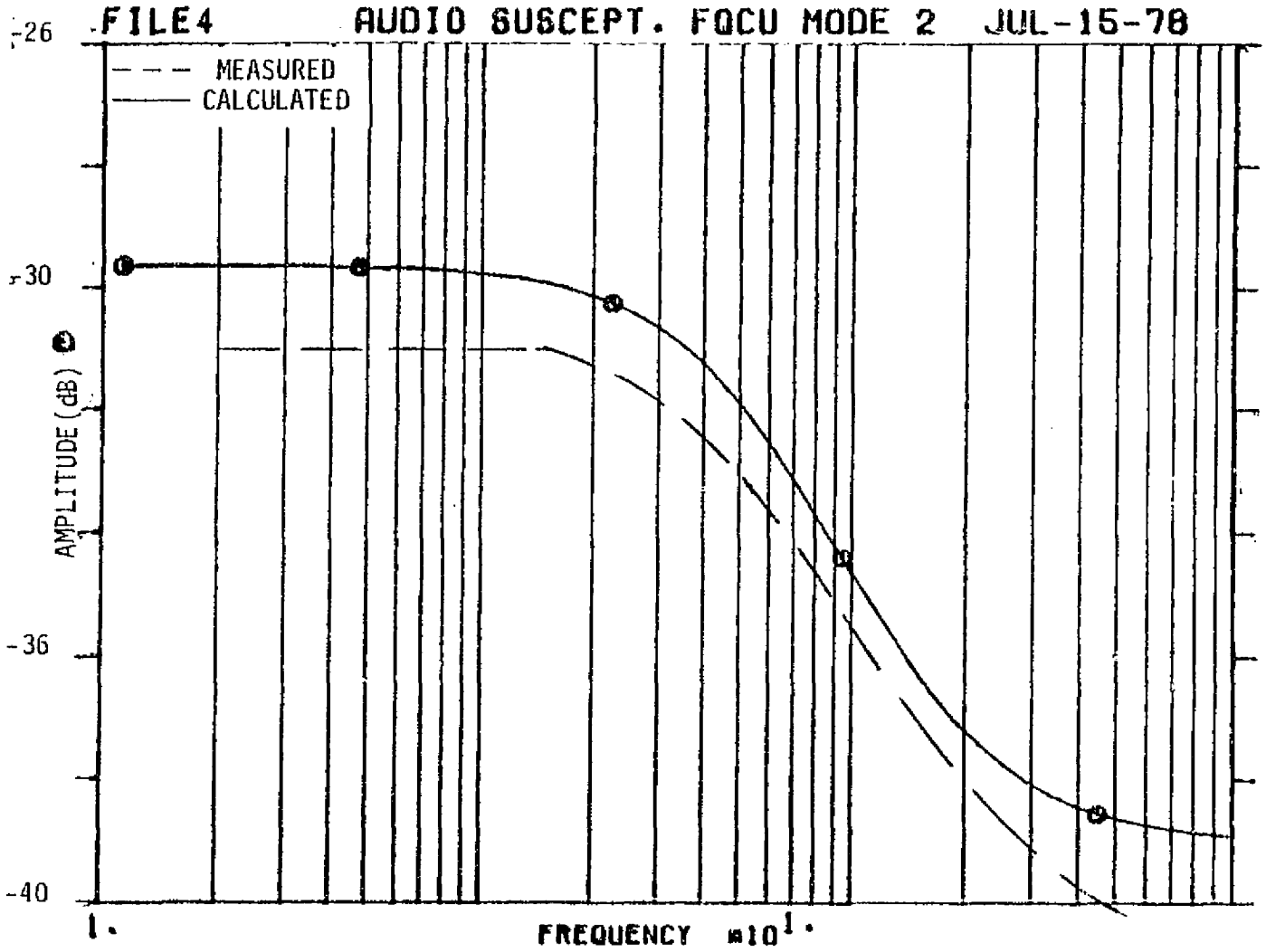

Figure 4.19 Audio susceptibility of a constant-frequency current step-up converter operating in the discontinuous conduction mode. Power stage of figure 4.2, controller of figure 2.2.

Discussion

Comparisons between the measured and calculated magnitude responses demonstrate good correlation in almost all cases. Most transfer functions are very close at low frequencies with marked discrepancies occuring only at frequencies above 1 kHz. As discussed in chapter II, the power stage transfer functions are applicable only to frequencies below half the switching fequency. In this case half the switching frequency is 5 kHz. It is possible that the power stage model does not approximate the system at these higher frequencies. A more feasible explanation lies in the modeling of the feedback controller. The controller is modeled in chapter II as being ideal with no frequency dependent elements. While this assumption is correct when speaking of the isolated controller, when the controller is placed in the closed-loop converter, effects due to the pulse-width-modulation scheme are present. These effects include sampling delays that have not been investigated or included in this thesis. A topic for further investigation would be the more careful characterization of the feedback controller. Even with this simple model for the feedback controller there is sufficient correlation between theory and experiment to consider both to be valid research tools.

The phase measurements shown in the four loop gain transfer functions deviate greatly at both high and low frequencies. These discrepancies can be attributed to the fact that the relative magnitudes of V_{xe} and V_{ye} at both high and low frequencies are separated enough to make the equation for the calculation of phase from the three voltage magnitudes V_{ze}, V_{xe}, and V_{ye} very sensitive to small changes in V_{xe} or V_{ye}. However, when

V_{xe} and V_{ye} are of comparable amplitude, that is to say near unity gain, the phase measurement shows good correlation with the theoretical phase angle. Phase margin can thus be obtained from the measurement scheme.

CHAPTER V

CONCLUSIONS

Procedures have been presented that can be used to obtain valid frequency-domain transfer functions of regulated reactor energy-storage dc-to-dc converters. The procedures presented are for the measurement of loop gain, closed-loop gain, output impedance, and audio susceptibility. Comparisons between results obtained by applying the physical measurement procedures and analytical transfer functions generated by a computer analysis program indicate that it is possible to obtain good correlation between experiment and theory. The loop gain measurements can be used to obtain magnitude and phase information which will provide phase margin for regulated dc-to-dc converters. It is therefore possible to determine the degree of stability of an existing converter. Closed-loop gain measurement are presented in a normalized form to allow meaningful comparisons between converters operating with different output voltages or reference voltages. Output impedance measurements give insight into the behavior of a dc-to-dc converter in different output environments. Procedures for the measurement of audio susceptibility can be used to obtain quantitative data concerning the behavior of the converter in an system having a noisy input voltage. Audio susceptibility is also presented in a normalized fashion to allow comparisons between converters operating at different voltage levels.

Caution must be exercised when applying the measurement procedures because it is quite possible to obtain a completely false measurement of a transfer function if certain portions of the procedures are ignored or misinterpreted. An effort has been made to make these experimental procedures as unambiguous as possible. If the steps of the procedure

section are closely followed and all warnings and precautions are observed true experimental data is easily taken.

The noisy switching environment is an interesting complication of the problem of measuring small-signal frequency-domain transfer functions. This is certainly an area of possible application of an instrument such as a wave analyzer which contains a sinusoidal oscillator section that is tracked by a frequency-band selective voltmeter. However, this is not the intended application of this instrument. A more likely candidate for use in the extraction of a small sinuoid from a noisy environment would be a lock-in analyzer. This instrument uses a cross-correlation scheme or similar approach to lock onto the frequency provided by a clean external sinusoidal oscillator and then to pluck the component of the same frequency from a waveform containing the signal plus noise. By using a lock-in analyzer equipped with the proper options, magnitude and phase information can be obtained for all of the transfer functions described in this thesis, whereas for all practical purposes, only magnitude information is available from the wave analyzer in all but one of the transfer functions.

Preliminary investigations using a lock-in analyzer instrument demonstrate better correlation than is reported in this thesis by using the wave analyzer. The procedures are still completely valid and the lock-in analyzer can be incorporated into the procedures with only slight modifications.

The lock-in analyzer instrument has a major drawback in that it is more expensive than a wave analyzer. It is for this reason that a lock-in analyzer was not available for the major portion of the research effort covered by this thesis. To the knowledge of the author and his research

associates the preliminary work conducted to date with the lock-in analyzer is quite possibly the first application of such an instrument to the measurement of the frequency-domain transfer functions in regulated dc-to-dc converters.

It is hoped that the procedures that are the principal subject of this thesis will provide a sound base for the future measurement and analysis of regulated dc-to-dc converters. It is also hoped that these procedures shed light into other areas of engineering where similar nonlinearities and/or noise complicate the measurement and characterization of systems in the frequency domain.

LIST OF REFERENCES